

Accepted Manuscript

Discovery of highly selective and potent monoamine oxidase B inhibitors: Contribution of additional phenyl rings introduced into 2-aryl-1,3,4-oxadiazin-5(6H)-one

Jungeun Lee, Yeongcheol Lee, So Jung Park, Joohee Lee, Yeong Shik Kim, Young-Ger Suh, Jeeyeon Lee



PII: S0223-5234(17)30144-7

DOI: [10.1016/j.ejmech.2017.02.059](https://doi.org/10.1016/j.ejmech.2017.02.059)

Reference: EJMECH 9255

To appear in: *European Journal of Medicinal Chemistry*

Received Date: 21 November 2016

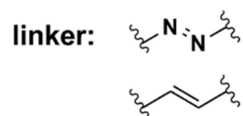
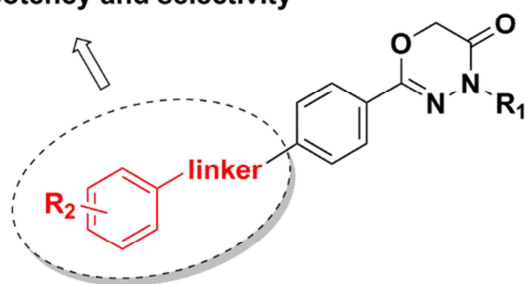
Revised Date: 23 January 2017

Accepted Date: 27 February 2017

Please cite this article as: J. Lee, Y. Lee, S.J. Park, J. Lee, Y.S. Kim, Y.-G. Suh, J. Lee, Discovery of highly selective and potent monoamine oxidase B inhibitors: Contribution of additional phenyl rings introduced into 2-aryl-1,3,4-oxadiazin-5(6H)-one, *European Journal of Medicinal Chemistry* (2017), doi: 10.1016/j.ejmech.2017.02.059.

This is a PDF file of an unedited manuscript that has been accepted for publication. As a service to our customers we are providing this early version of the manuscript. The manuscript will undergo copyediting, typesetting, and review of the resulting proof before it is published in its final form. Please note that during the production process errors may be discovered which could affect the content, and all legal disclaimers that apply to the journal pertain.

Increase potency and selectivity



18a, 18b, 18e and 25b

IC₅₀ = 4–25 nM

SI > 4000

2-Aryl-4H-1,3,4-oxadiazin-5(6H)-one scaffold

ACCEPTED MANUSCRIPT

Discovery of highly selective and potent monoamine oxidase B inhibitors: contribution of additional phenyl rings introduced into 2-aryl-1,3,4-oxadiazin-5(6H)-one

Jungeun Lee, Yeongcheol Lee, So Jung Park, Joohee Lee, Yeong Shik Kim, Young-Ger Suh,
and Jeeyeon Lee*

*College of Pharmacy and Research Institute of Pharmaceutical Sciences, Seoul National
University, Seoul 08826, Korea*

* Corresponding author.

E-mail address: jyleeut@snu.ac.kr (J. Lee).

Abstract

Monoamine oxidase B (MAO-B) is a flavin adenine dinucleotide (FAD)-containing enzyme that plays a major role in the oxidative deamination of biogenic amines and neurotransmitters. Inhibiting MAO-B activity is a promising approach in the treatment of neurological disorders. Here, we report a series of 2-aryl-1,3,4-oxadiazin-5(6*H*)-one derivatives as highly selective and potent MAO-B inhibitors. Analysis of the binding sites of hMAO-A and hMAO-B led to design of linear analogs of 2-aryl-1,3,4-oxadiazin-5(6*H*)-one with an additional phenyl ring. Biological evaluation of the 26 new derivatives resulted in the identification of highly potent and selective inhibitors with optimal physicochemical properties to potentially cross the blood-brain barrier (BBB). Compounds **18a**, **18b**, **18e** and **25b** potently inhibited MAO-B, with IC₅₀ values of 4–25 nM and excellent SI over MAO-A (**18a** > 25000, **18b** > 8333 and **18e** > 4000 and **25b** > 4545). Docking results suggest that an optimal linker between two aromatic rings on the 2-aryl-1,3,4-oxadiazin-5(6*H*)-one scaffold is a key element in the binding and inhibition of MAO-B.

1. Introduction

Monoamine oxidase (MAO), a flavin adenine dinucleotide (FAD)-containing enzyme, catalyzes the oxidative deamination of a range of biogenic amines and monoamine neurotransmitters. Two isoforms of MAO (MAO-A and MAO-B) are present in most mammalian tissues, with the two distinguished by their tissue distribution and substrate/inhibitor preference [1-3]. Serotonin (5-HT) and noradrenaline (NE) are the preferred substrates of MAO-A, whereas phenethylamine (PEA) and benzylamine exhibit higher affinity toward MAO-B. Dopamine (DA) and tyramine are oxidized by both isoforms [3-5]. Most mammalian peripheral tissues express both isoforms, but the proportions of MAO vary among tissues. Human placenta expresses MAO-A, whereas platelets and brain have high levels of MAO-B [6-8].

The ability of MAO to control the levels of several neurotransmitters, mainly in the central nervous system (CNS), attracted the attention of many researchers, leading to the discovery of new drugs targeting brain disorders [9-17]. MAO-A inhibitors are used in the treatment of depression [18, 19], whereas selective MAO-B inhibitors, combined with levodopa, are used to treat early Parkinson's disease (PD), reducing the metabolic degradation of DA [20-23]. MAO-B activity in human brain increases with age [24, 25], because of the predominant expression of MAO-B in glial cells [26]. Controlling the level of MAO-B activity may influence susceptibility to neurodegenerative diseases, including Alzheimer's disease (AD) and PD [27, 28]. The increased level of DA oxidation by MAO-B in the elderly is related to the loss of dopaminergic neurons in the substantia nigra and has been observed in patients with PD [29].

The earliest non-selective and irreversible inhibitors of MAOs showed severe side effects, including tyramine-induced hypertensive crisis (Cheese reaction) [30, 31]. Therefore, research on additional MAO inhibitors has focused on their selectivity for the two isoforms, MAO-A and MAO-B [32-42]. Clorgyline (**1**) in Fig. 1 is a potent and selective inhibitor of MAO-A [43-45], whereas selegiline (**2**) and rasagiline (**3**) are selective irreversible inhibitors of MAO-B and are FDA-approved drugs for PD [46-49]. Safinamide (**4**) is a selective and reversible inhibitor of MAO-B recently approved by

the European Commission as an add-on therapy to levodopa or in combination with other medications to treat patients with PD [22, 50]. Compounds **5–7** are previously reported inhibitors of MAO-B, with IC_{50} values in the low nanomolar range [35, 38, 39].

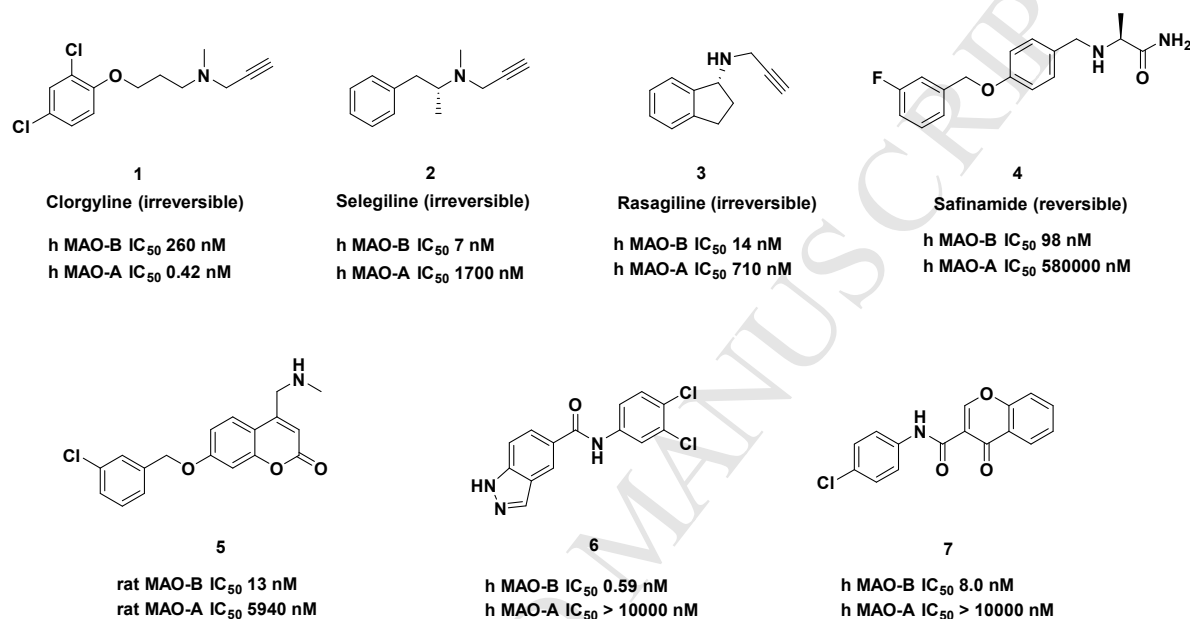
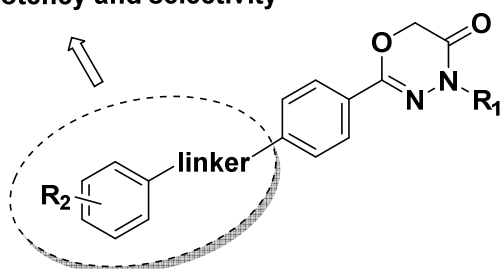


Fig. 1. Structures of MAO inhibitors and potencies of previously reported MAO-B inhibitors.

Our research group has explored nitrogen-containing heterocycle scaffolds, including 1,3,4-oxadiazin-5(6*H*)-one scaffolds, to extend their activity profiles [51]. Although analogs of 1,3,4-oxadiazin-5(6*H*)-one have been previously shown to act as MAO inhibitors [52-55], selective inhibitors of human MAO-B have not yet been explored. Here, we describe a new class of MAO-B inhibitors, constructed using a 2-aryl-4*H*-1,3,4-oxadiazin-5(6*H*)-one scaffold, with enhanced potency and selectivity. Based on the structural features of MAO-A and MAO-B, we envisioned that selectivity toward MAO-B could be achieved by introducing another phenyl ring and a linker unit connecting two phenyl rings (Fig. 2). In this study, we describe the design and synthesis of a new series of 2-aryl-4*H*-1,3,4-oxadiazin-5(6*H*)-one compounds with various linkers, along with their

ability to inhibit the activity of human MAO enzymes. In addition, we describe molecular docking studies to predict the mode of binding and interactions of selected compounds with MAO-B.

Increase potency and selectivity



2-Aryl-4H-1,3,4-oxadiazin-5(6H)-one scaffold

Fig. 2. Design strategy to obtain potent and selective inhibitors of MAO-B.

2. Results and discussion

2.1. Design and synthesis

To develop MAO-B selective inhibitors, we started by comparing the binding sites of hMAO-A (PDB code 2BXR) [56] and hMAO-B (PDB code 2V5Z) [57], based on their reported protein structures (Fig. 3). Although the overall structures of the two isoenzymes (MAO-A and MAO-B) are similar, there are major differences in their active sites, which have different shapes and sizes [56]. The active site of hMAO-B consists of two cavities, an entrance cavity with a volume of 290 \AA^3 and a larger substrate cavity with a volume of 420 \AA^3 , resulting in a longer and narrower cavity than that of hMAO-A. By contrast, hMAO-A has a single substrate cavity of $\sim 550 \text{ \AA}^3$, which is less flat and less elongated than the substrate cavity of hMAO-B [9, 56-58]. In designing selective MAO-B inhibitors, we initially hypothesized that an additional phenyl ring on the 2-aryl-1,3,4-oxadiazin-

5(6*H*)-one scaffold may contribute to selectivity for hMAO-B, owing to its longer and narrower active site with two cavities, and may increase the potency of inhibitors by occupying both cavities of MAO-B (Fig. 2).

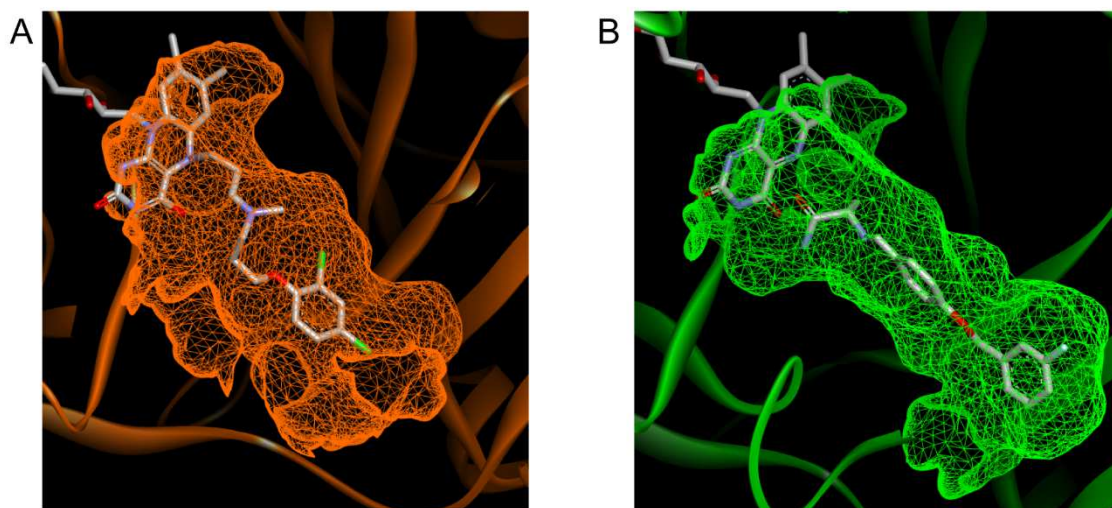
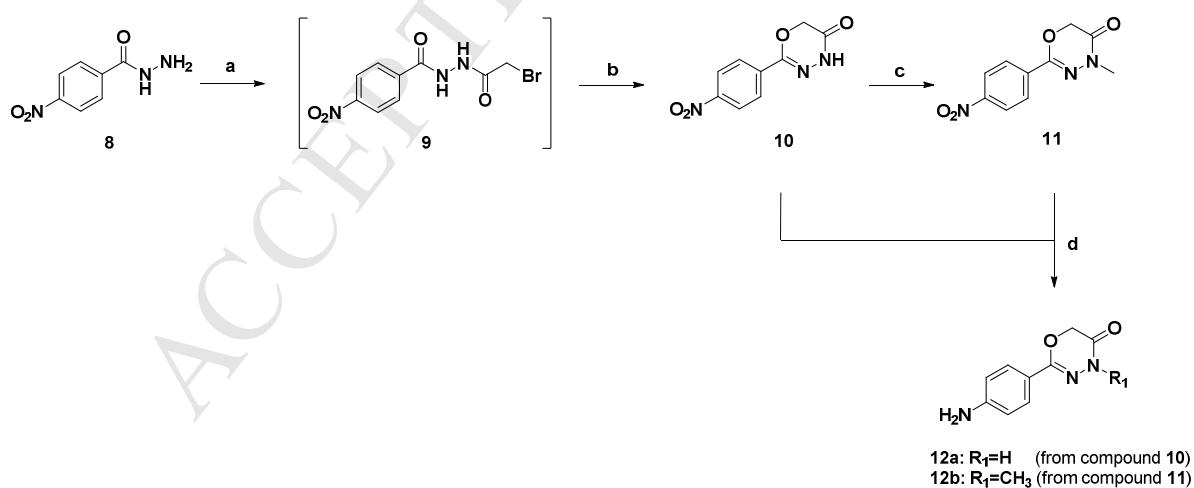


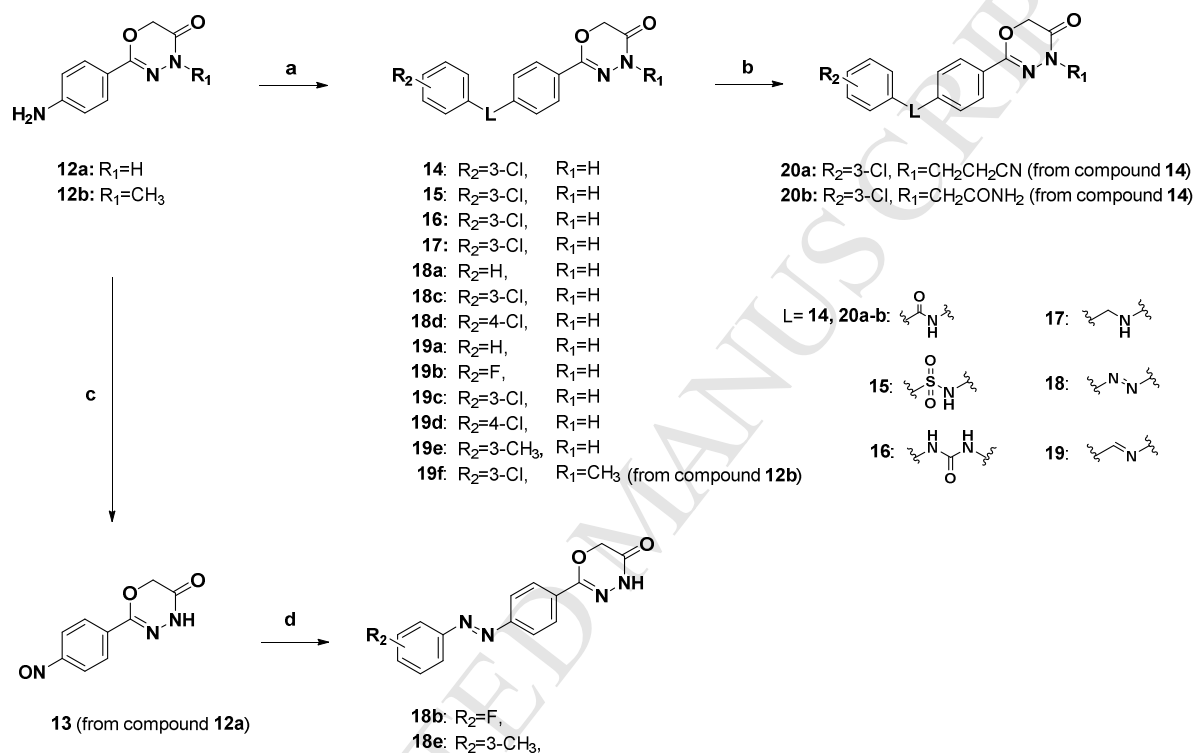
Fig. 3. Active site of human MAO-A (A, PDB: 2BXR, co-crystallized with clorgyline) and MAO-B (B, PDB: 2V5Z, co-crystallized with safinamide).

Most of compounds in the present study were synthesized as described in Schemes 1–3, with the synthetic routes of **31**, **39**, **40** and **25f** presented in the Supporting information. In general, the 1,3,4-oxadiazine-5(6*H*)-one ring was synthesized by amide coupling of hydrazide with bromoacetic acid, followed by a cyclization reaction in the presence of *N,N*-diisopropylethylamine (DIEA) (Scheme 1). The key intermediate **12** was obtained by nitro reduction of **10** or **11** in the presence of stannous chloride as a reducing agent. After obtaining the common intermediate, a variety of linker units were introduced between the two benzene rings to investigate the impact of the linker on inhibitory activity (Scheme 2). These linker units included amide (**14**), sulfonamide (**15**), urea (**16**), alkyl amine (**17**), azo (**18**), imine (**19**), olefin (**25**), inverse amide (**31**), inverse imine (**39**) and hydrazine

(40) linkers. The final products **14–19** were prepared by reacting **12a** with their corresponding reagents. The intermediate **12a** or **13** was reacted with differently substituted reagents at the R₂ position to yield **18a–e** and **19a–e**. Nitrosobenzene **13** was obtained by oxidation of aniline **12a** with hydrogen peroxide, catalyzed by molybdenum oxide (MoO₃), with **13** subsequently reacted with 3-fluoroaniline or *m*-toluidine to generate **18b** or **18e** with azo linkers. The derivatives of an olefin linker were prepared as depicted in Scheme 3. Compounds **22a–e** were prepared by Horner–Wadsworth–Emmons reaction of aldehyde reagent **21** with commercially available phosphonates. Reacting **22** with excess hydrazine hydrate in ethanol yielded compound **23**. The final compounds **25a–e** were synthesized by the general procedure described in Scheme 1 for the synthesis of the 1,3,4-oxadiazine-5(6*H*)-one scaffold. Reaction conditions and compound characterization are described in the Experimental section. In NMR spectra, the imine peak for **19c** was shown at 8.67 ppm, whereas *trans* olefin of stilbene moiety of **25d** appeared at 7.36 and 7.31 ppm with the *J* value of 16.4 Hz (Supporting). For **18a** with the diazo linker, protons adjacent to the azo group were merged to 8.00-7.91 ppm shown as multiplets

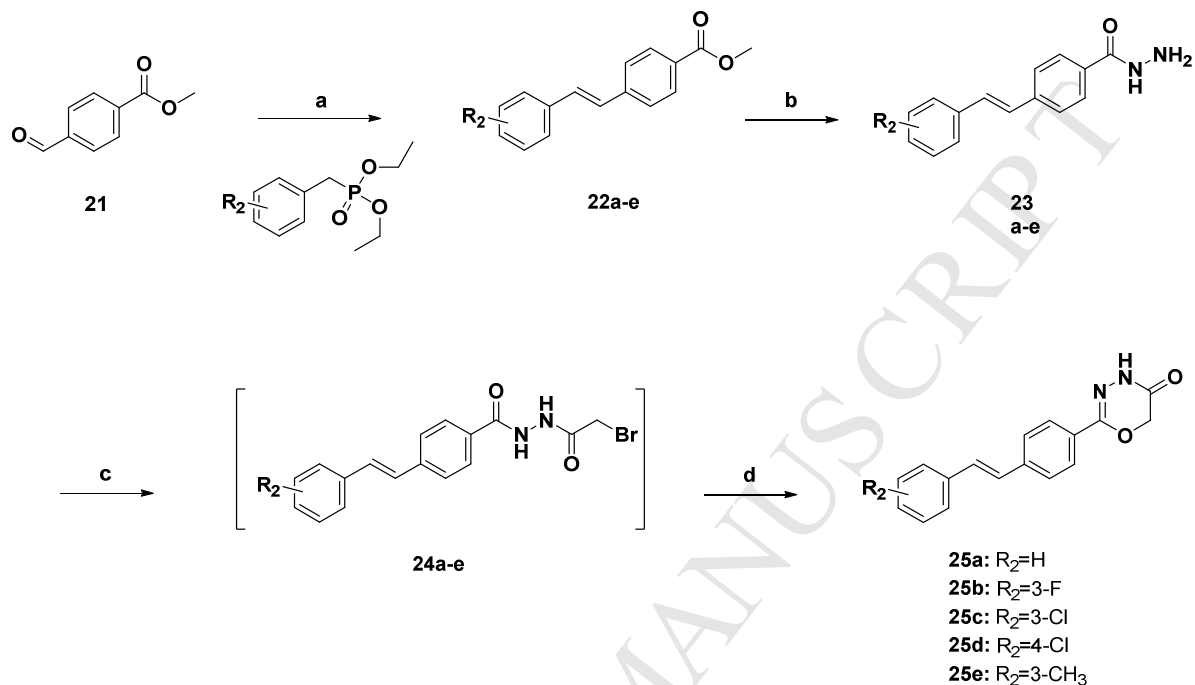


Scheme 1. Reagents and conditions: a) Bromoacetic acid, EDCl, DMF, rt, 1 h; b) DIEA, DMF, 60 °C, 12 h, yield 68% in 2 steps; c) Methyl iodide, NaH, DMF, rt, 1.5 h, yield 67%; d) SnCl₂·2H₂O, DMF, 70 °C, 1 h, yields 80% (**12a**) and 90% (**12b**).



Scheme 2. Reagents and conditions: a-1) 3-Chlorobenzoyl chloride, Et₃N, DMF, rt, 1 h (for compound **14**), yield 35% in 2 steps; a-2) 3-Chlorobenzenesulfonyl chloride, pyridine, 0 °C, 1 h (for compound **15**), yield 60%; a-3) 3-Chlorophenyl isocyanate, DCM/DMF, rt, 12 h (for compound **16**), yield 53%; a-4) 3-Chlorobenzaldehyde, NaCNBH₄, MeOH, 1% acetic acid, rt, 2 h (for compound **17**), yield 75%; a-5) 3- or 4- Substituted nitrosobenzene, acetic acid, rt, 12 h (for compound **18**), yield 78–86%; a-6) 3- or 4- Substituted benzaldehyde, EtOH, reflux, 12 h (for compound **19**), yield 45–80%; b) 3-Bromopropionitrile (for compound **20a**) or 2-chloroacetamide (for compound **20b**), NaH, DMF, rt, 1 h, yield 95% (**20a**) and 72% (**20b**); c) MoO₃, H₂O₂, H₂O, MeOH, rt, 5 d, yield

85%; d) 3-Fluoroaniline (for compound **18b**) or *m*-toluidine (for compound **18e**), acetic acid, rt, 12 h, yield 69% (**18b**) and 31% (**18e**).



Scheme 3. Reagents and conditions: a) 3- or 4- Substituted diethyl benzylphosphonate, NaH, THF, rt, 1 h, yield 50–85% ; b) Hydrazine monohydrate, EtOH, reflux, 12 h, yield 44–77%; c) Bromoacetic acid, EDCI, DMF, rt, 1 h; d) DIEA, DMF, 70 °C, 1 d, yield 24–26% in 2 steps.

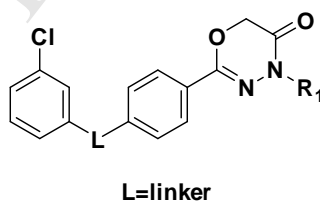
2.2. In vitro inhibition of MAO

All the synthesized analogs of 1,3,4-oxadiazin-5(6*H*)-one were tested for inhibition of human MAO-A and MAO-B activity. The corresponding IC₅₀ values and selectivity indices of these compounds relative to MAO-B are shown in Tables 1–3. The ability of these compounds to inhibit the enzymatic activities of hMAO-A and hMAO-B was tested by measuring the production of hydrogen peroxide (H₂O₂) from *p*-tyramine using a fluorescence-based assay kit (see Experimental section) [59]. The biological evaluation of 26 new derivatives resulted in the identification of highly potent and selective inhibitors of MAO-B.

First, we examined 10 derivatives that included various linkers between two phenyl rings, including amide (**14**), sulfonamide (**15**), urea (**16**), alkyl amine (**17**), azo (**18c**), imine (**19c**), olefin (**25c**), inverse amide (**31**), inverse imine (**39**) and hydrazine (**40**) linkers (see Table 1). In general, linkers containing a π bond between two atoms ($\text{Ar-X}=\text{X-Ar}$, $\text{X}=\text{C}$ or N , **18c**, **19c**, **25c** and **39**) showed good inhibitory activities against MAO-B, with IC_{50} values of 287 nM, 257 nM, 173 nM, and 551 nM, respectively. Introduction of one more atom between the two phenyl groups (**16** and **40**) or bulky linker units such as sulfonamide (**15**) and urea (**16**) reduced the inhibitory activity against MAO-B compared with the smaller linkers. Introduction of a flexible linker (**17**, $\text{IC}_{50} = 2690$ nM) dramatically reduced the inhibitory effect against MAO-B when compared with rigid linkers (**18c**, **19c** and **25c**). These results indicate that proper linker units with optimal distance between two aromatic units are essential for inhibiting MAO-B. Introduction of an alkyl substituent at the R_1 position of the 1,3,4-oxadiazin-5(6H)-one ring significantly reduced inhibitory activities when compared with unsubstituted compounds (**20a**, **20b** vs **14**; **19f** vs **19c**; **25f** vs **25c**).

Table 1

In vitro activities on hMAO of 1,3,4-oxadiazinone derivatives: Variation of linker or R_1 position.



Compd.	Linker	R_1	hMAO-B (IC_{50} , nM) ^a	hMAO-A (IC_{50} , nM) ^a	SI^b
14		H	284 ± 14	>100000	> 357
15		H	>10000	>100000	nd
16		H	2891 ± 234	>100000	> 34

17		H	2690 ± 144	>100000	>37
18c		H	287 ± 200	>100000	> 348
19c		H	257 ± 49	>100000	> 385
25c		H	173 ± 17	>100000	> 578
31		H	288 ± 21	>100000	> 344
39		H	551 ± 133	>100000	> 182
40		H	554 ± 45	>10000	>18
20a		CH ₂ CH ₂ CN	4228 ± 199	>100000	> 24
20b		CH ₂ CONH ₂	3692 ± 538	>100000	> 27
19f		CH ₃	2033 ± 420	>100000	> 49
25f		CH ₂ CH ₃	>10000	>100000	nd

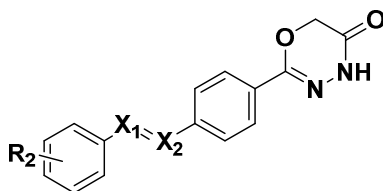
^aEach IC₅₀ value is the mean ± standard error of the mean (SEM) of more than three independent experiments. ^bSelectivity index. It was calculated as IC₅₀(hMAO-A)/ IC₅₀(hMAO-B).

Notably, all of the compounds listed in Table 1 exhibited higher inhibitory activities against MAO-B than MAO-A. Most compounds did not show any inhibitory effects on MAO-A at 100 μM concentrations, except for **40**. Based on the first structure-activity relationship (SAR) analysis, we selected three compounds with relatively small linkers having a π bond with good inhibitory activities against MAO-B (**18c**, IC₅₀ = 287 nM; **19c**, IC₅₀ = 257 nM; **25c**, IC₅₀ = 173 nM) for further optimization.

To further explore the effect of substitutions at the R₂ position of the first phenyl ring, we prepared R₂ substituted analogs with azo, olefin and imine linkers (Tables 2 and 3). We compared the effects of 4-Cl and 3-Cl substituted series on MAO-B activity to evaluate the contribution of meta or para substitution (Table 2). Because the compounds with 3-Cl substitution (**18c**, **25c** and **19c**) at the R₂ position had slightly more potent inhibitory activities against MAO-B than those with 4-Cl substitution (**18d**, **25d** and **19d**), we fixed the substituent at the meta position of the phenyl ring.

Table 2

In vitro activities on hMAO of 1,3,4-oxadiazinone derivatives: meta or para substitution at R₂ position.



Compd.	R ₂	X ₁ =X ₂	hMAO-B (IC ₅₀ , nM) ^a	hMAO-A (IC ₅₀ , nM) ^a	SI ^b
18c		N=N	287 ± 200	>100000	> 348
25c	3-Cl	C=C	173 ± 17	>100000	> 578
19c		C=N	257 ± 49	>100000	> 385
18d		N=N	392 ± 47	>100000	> 255
25d	4-Cl	C=C	542 ± 111	>100000	> 185
19d		C=N	433 ± 35	>100000	> 231

^aEach IC₅₀ value is the mean ± SEM of more than three independent experiments. ^bSelectivity index.

It was calculated as IC₅₀(hMAO-A)/ IC₅₀(hMAO-B).

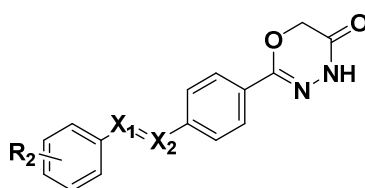
Interestingly, H, 3-F and 3-CH₃ analogs significantly differed in inhibitory activities against MAO-B among the three linkers, azo, olefin and imine (Table 3). In general, the potency of 3-H, 3-F and 3-CH₃ derivatives increased in the order of imine < olefin < azo. Compounds with azo linkers (**18a**, **18b** and **18e**) showed greater inhibition of MAO-B than did compounds with olefin or imine linkers. In addition, compounds with a small (F) or no substituent at the meta position (**18a**, **18b** and **25b**) were more potent inhibitors in the presence of azo or olefin linkers, with IC₅₀ values of 4, 12, and 22 nM, respectively. These results indicate that the steric effect of the R₂ group in the presence of an

azo or olefin linker plays a key role in the modulation of MAO-B inhibitory activity. Interestingly, the azo derivative with 3-CH₃ (**18e**) was 10-fold more active than the derivative with 3-Cl (**18c**). The hydrophobic property of 3-CH₃ in the azo series may be responsible for its increased potency because of hydrophobic environments of the active site of human MAO-B [57]. None of the compounds in Table 3 inhibited MAO-A at 100 μ M concentrations. Compounds with azo linkers and 3-H, 3-F and 3-CH₃ substituents at the R₂ position (**18a**, **18b** and **18e**) and an olefin derivative with a 3-F substituent at R₂ (**25b**) showed increased potency and selectivity, with IC₅₀ values of 4–25 nM and selectivity indices (SI) greater than 4000. Compared with the current MAO-B inhibitors (selegiline, IC₅₀ = 7 nM; rasagiline, IC₅₀ = 14 nM; safinamide, IC₅₀ = 98 nM) [47, 50], these compounds have similar or more potent activities, along with excellent SIs.

To determine the binding mode of studied compounds, a time-dependency of enzyme inhibition was measured. If the compounds form covalent adduct with the enzyme, a time-dependent reduction of enzyme activity would be expected. **18a**, **25b**, **19c**, and **19e** were preincubated with MAO-B for 0, 15, 30, and 60 mins prior to starting the enzyme reaction. As shown in Figure 4, enzyme activity was not reduced with increased preincubation time, indicating that selected compounds were reversible inhibitors of MAO-B. Based on the Lineweaver-Burk plots (Figure S1), the selected compounds are likely to be competitive MAO-B inhibitors.

Table 3

In vitro activities on hMAO of 1,3,4-oxadiazinone derivatives: R₂ variation with selected linkers.



Compd.	X ₁ =X ₂	R ₂	hMAO-B (IC ₅₀ , nM) ^a	hMAO-A (IC ₅₀ , nM) ^a	SI ^b
18a		H	4 ± 3	>100000	> 25000
18b	N=N	3-F	12 ± 10	>100000	> 8333
18e		3-CH ₃	25 ± 5	>100000	> 4000
25a		H	165 ± 95	>100000	> 606
25b	C=C	3-F	22 ± 1	>100000	> 4545
25e		3-CH ₃	338 ± 47	>100000	> 296
19a		H	>10000	>100000	nd ^c
19b	C=N	3-F	1526 ± 91	>100000	> 65
19e		3-CH ₃	1270 ± 229	>100000	> 78
Clorgyline ^d (1)			61350 ^e	4 ^e	
Selegiline (2)			7 ^f	1700 ^f	242
Rasagiline (3)			14 ^f	710 ^f	50
Safinamide ^d (4)			6 ± 3		
			98 ^g	580000 ^g	5918

^aEach IC₅₀ value is the mean ± SEM of three independent experiments. ^bSelectivity index. It was calculated as IC₅₀(hMAO-A)/ IC₅₀(hMAO-B). ^cNot determined. ^dPositive controls; safinamide: reversible MAO-B inhibitor, clorgyline: irreversible MAO-A inhibitor. ^eValues reported in ref 44. ^fValues reported in ref 47. ^gValues reported in ref 50.

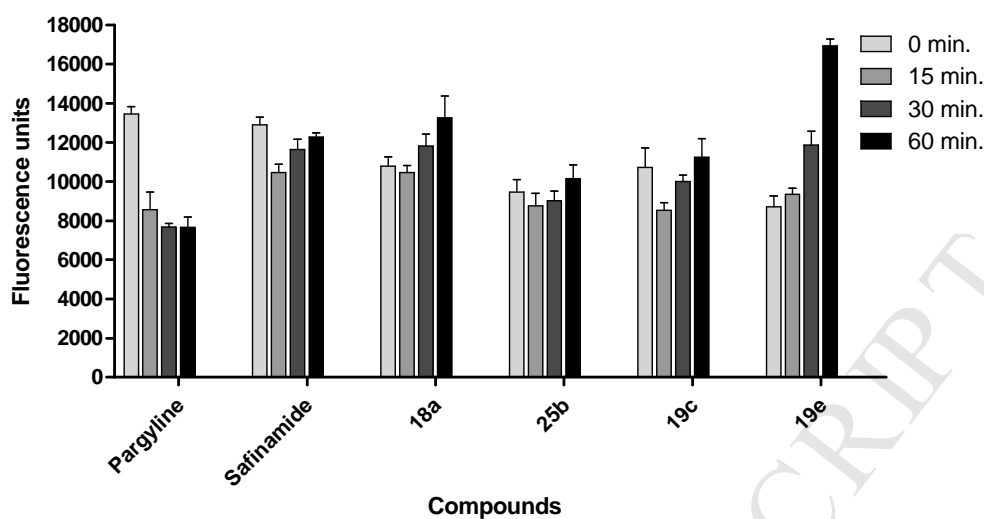


Fig. 4. Time dependency of MAO-B inhibition in the presence of **18a**, **25b**, **19c**, and **19e**. Data are expressed as the mean \pm SEM of three independent experiments.

2.3. Molecular docking

To understand the possible binding mode of the synthesized compounds, we performed flexible docking simulations of azo linker compounds (**18a** and **18b**) and imine derivatives (**19a** and **19b**), using the X-ray cocrystal structure of human MAO-B with safinamide (**4**, PDB code 2V5Z, see Experimental section) [57]. All the tested ligands (**18a**, **18b**, **19a** and **19b**) occupied both the substrate and entrance cavities in the active site of MAO-B. The 4H-1,3,4-oxadiazin-5(6H)-one ring, the relatively polar part of these molecules, was oriented in the substrate cavity toward FAD, whereas the two phenyl rings were directed towards the hydrophobic pocket in the entrance cavity. Potential interactions with the gate residues (Leu171 and Ile199) may have resulted in compounds residing in both cavities [9]. Docking results in Fig. 5 showed that compounds containing an azo group (**18a** and **18b**) appeared to properly occupy the hydrophobic entrance pocket by interacting with Leu164, Leu171, Ile199, Ile316 and Tyr326. In particular, Tyr326, a critical residue in the recognition of inhibitors [60-62], exhibits a π - π interaction with the phenyl group in the middle. The compounds **18a** and **18b** were also stabilized by hydrogen bonding interactions between the N-H of

the 4H-1,3,4-oxadiazin-5(6H)-one ring and the carbonyl group of Cys172 (Fig. 5A and D). In addition, the π -sulfur interaction with Cys172 appears to play an important role. In contrast, compounds with imine linkers (**19a** and **19b**) do not exhibit hydrogen-bonding interactions with Cys172, shifting them towards the FAD binding side (Fig. 5B and E). Consequently, these compounds may not well fit into the buried hydrophobic pocket in the entrance cavity. These docking results suggest that optimizing the linker between the two aromatic rings is a key element in the binding to and inhibition of MAO-B.

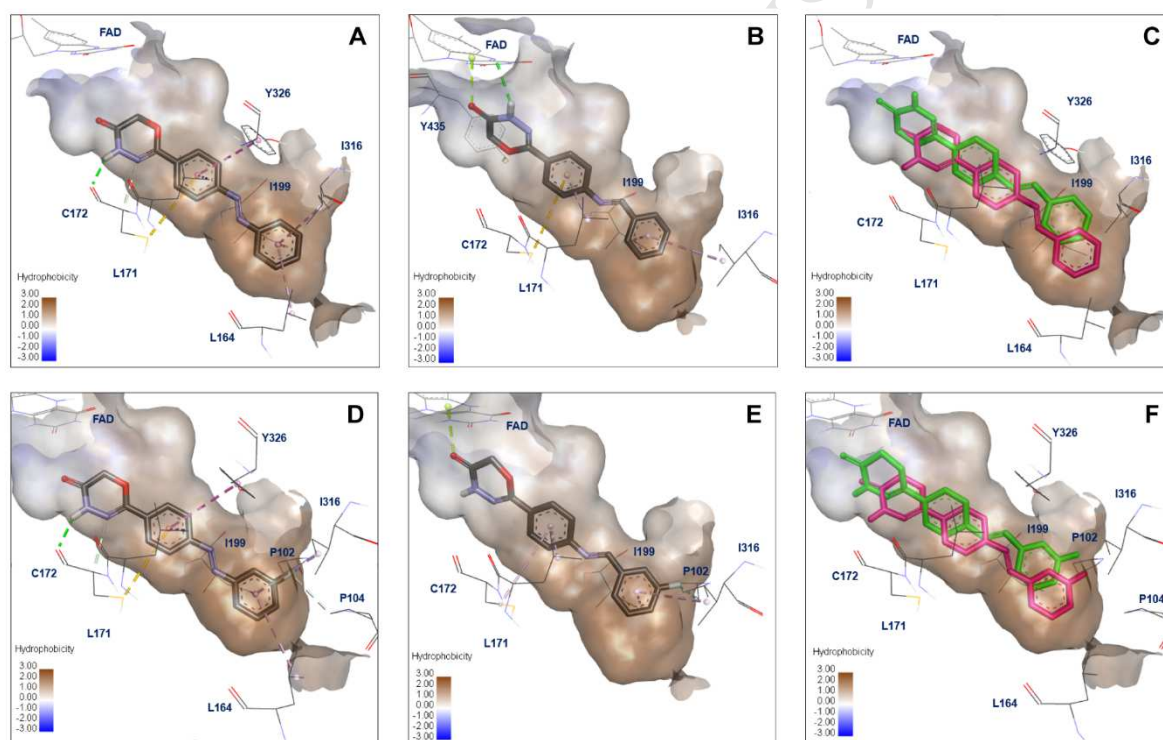


Fig. 5. Predicted binding mode of **18a** (A), **19a** (B), **18b** (D) and **19b** (E) in the human MAO-B (PDB code: 2V5Z) active site. (C) Overlaid structure of **18a** (magenta) and **19a** (green). (D) Overlaid structure of **18b** (magenta) and **19b** (green). Only the relevant residue side chains are shown.

2.4. Physicochemical properties

To understand the overall properties of the described derivatives, we calculated several physicochemical parameters, including lipophilicity (ClogP) and topological polar surface area (tPSA). The ClogP value of all compounds was lower than 5 and the molecular weight of all compounds was lower than 500, in agreement with Lipinski's rule-of-5 for drug-likeness [63]. The tPSA value of all analogs were within the *OK* ($140 > \text{PSA} > 61 \text{ \AA}^2$) or *good* range ($\text{PSA} \leq 61 \text{ \AA}^2$) for intestinal absorption [64]. In particular, compounds with an olefin linker (black dot) exhibited optimal tPSA value for good intestinal absorption ($\text{PSA} \leq 61 \text{ \AA}^2$) [64]. To further evaluate their ability to cross the blood-brain barrier (BBB), we selected four inhibitors (**18a**, **18b**, **18e** and **25b**) with high potency toward MAO-B, as shown by IC_{50} values $< 100 \text{ nM}$ (Table 4). Properties used to evaluate the ability of compounds to cross the BBB included ClogP, MW, tPSA and numbers of hydrogen bond donors (HBD). The physicochemical properties of selected compounds (**18a**, **18b**, **18e** and **25b**) were within the *suggested* limits ($\text{clogP} = 2\text{--}5$, $\text{PSA} < 90 \text{ \AA}^2$, $\text{MW} < 500$, $\text{HSD} < 3$) and compound **25b** were in the *preferred* range for BBB penetration ($\text{clogP} = 2\text{--}4$, $\text{PSA} < 70 \text{ \AA}^2$, $\text{MW} < 450$, $\text{HSD} = 0\text{--}1$) (Fig. 6.) [65]. Their tPSA values ranged between 50.4 and 73.0 and their MW was lower than that of the reference drug, safinamide. The tPSA values of the compounds in Fig. 6 were mainly determined by the linkers of these molecules. These results indicate that the linker moiety of the structure may be a critical element affecting the physicochemical properties as well as the potency of MAO-B inhibitors.

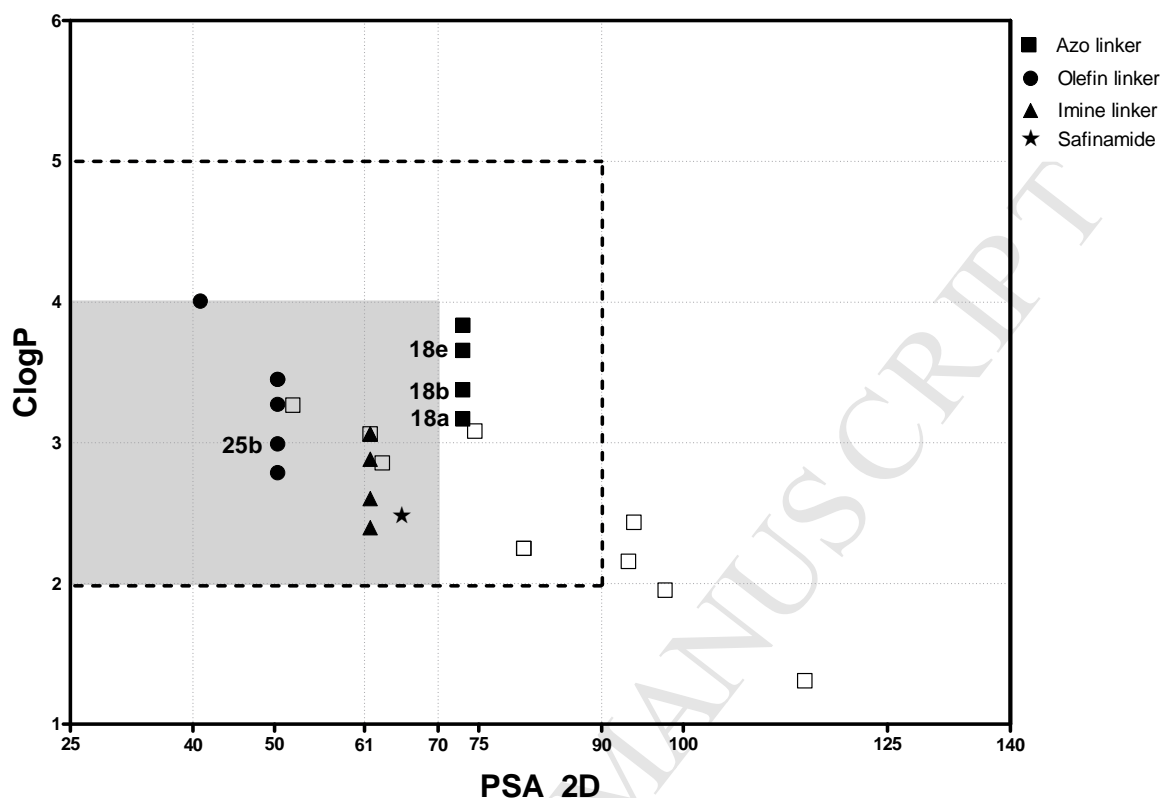


Fig. 6. Calculated physicochemical properties of the all tested compounds. *Preferred* range for crossing BBB is shown in gray color. *Suggested* limits for crossing BBB are shown in the dashed box.

Table 4

Calculated physicochemical properties of selected compounds and reference molecule

Compd.	hMAO-B inhibition (IC ₅₀ , nM)	Molecular weight	ClogP	tPSA	H-bond donors
18a	4	280.30	3.17	73.0	1
18b	12	298.28	3.38	73.0	1
18e	25	294.31	3.66	73.0	1

25b	22	296.30	2.99	50.4	1
Safinamide	6	302.34	2.48	65.6	2

2.5. Cytotoxicity assay

Cytotoxicity of 18a, 25b, 19c, and 19e toward PC-12, PC-12 Adh, and SH-SY5Y cells were measured at 10 and 50 μM using the WST-1 assay. PC-12 cells which are neuroblastoma cells were used because they are similar to dopaminergic neurons. Cell viability was not significantly reduced with the tested compounds except with 25b. More than 90% of cells were viable after treatment of 18a, 25b, 19c, and 19e, indicating low toxicity of studied compounds at higher concentration (50 μM). We also tested neuroprotective effect of the selected compounds (Figure S2). 5 μM rotenone or 150 μM H_2O_2 were treated to induce neurotoxicity, but no significant neuroprotective effect was observed. Further optimization for screening condition along with additional synthesis of derivatives based on oxadiazin-5(6H)-one scaffold will be pursued soon to discover neuroprotective agents.

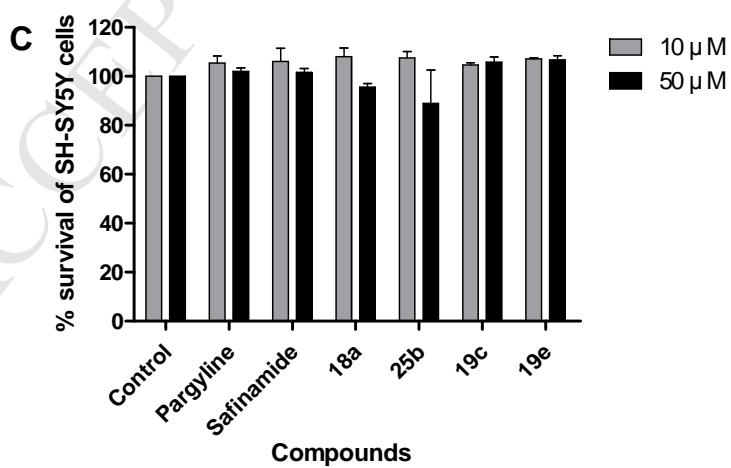
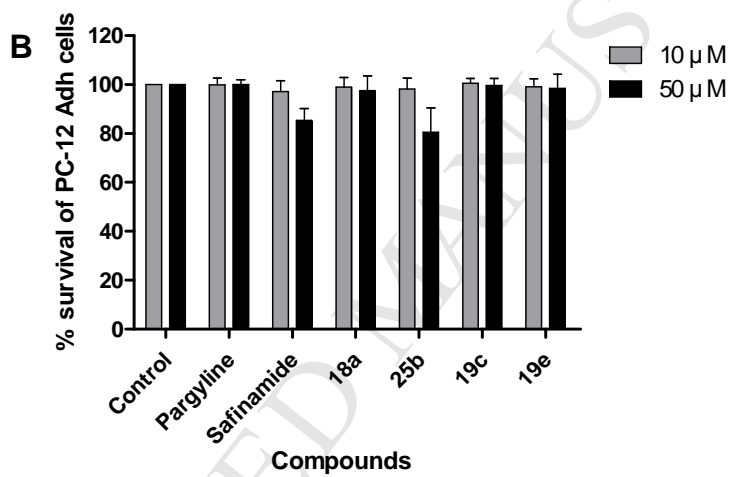
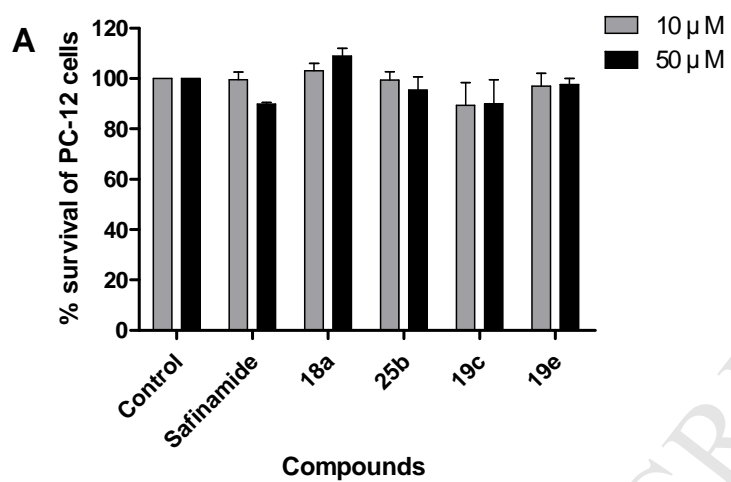


Fig. 7. Cytotoxicity of the representative compounds against PC-12 (A), PC-12 Adh (B), and SH-SY5Y (C) cells. Data are expressed as a percentage of control (\pm S.E.M, $n = 3$ in triplicate). Untreated cells were used as control.

3. Conclusion

We have identified new derivatives of 2-aryl-4H-1,3,4-oxadiazin-5(6H)-one as selective MAO-B inhibitors. Structural modification and analysis of SAR led to the identification of inhibitors with low nanomolar potency and excellent SI. The compounds with 3-H, 3-F and CH₃ substituents at the R₂ in azo compounds (**18a**, **18b** and **18e**) and a 3-F substituent at R₂ in an olefin derivative (**25b**) potently inhibited MAO-B with IC₅₀ values of 4–25 nM and excellent SIs (**18a** > 25000, **18b** > 8333 and **18e** > 4000 and **25b** > 4545). Molecular docking with the compounds containing azo (**18a** and **18b**) and imine (**19a** and **19b**) linkers provided insights into the main interactions and the importance of linker units for enzyme-inhibitor binding. Furthermore, the molecules with high potency, as shown by lower IC₅₀ values, had optimal calculated physicochemical properties allowing oral administration and BBB penetration. Notably, the tPSA values of 4H-1,3,4-oxadiazin-5(6H)-one derivatives were mainly affected by the linkers. Together with the SAR findings, the docking simulations and physicochemical properties suggested that the linker modification of the 2-aryl-4H-1,3,4-oxadiazin-5(6H)-one scaffold is a major strategy to optimize the potency and properties of a new class of MAO-B inhibitors.

4. Experimental procedures

4.1. Chemistry

Starting materials, reagents and solvents were purchased from Alfa aesar (Ward Hill, MA, USA), TCI (Tokyo, Japan) and Sigma-Aldrich (St. Louis, MO, USA). Melting points were determined on B-540 melting point analyzer (Buchi, Postfach, Flawil, Switzerland). ¹H NMR spectra (300, 400 MHz) and ¹³C NMR (75, 100, 125, 200 MHz) were recorded on GEMINI 2000 (VARIAN, Palo

Alto, CA, USA), JNM-LA300 (JEOL, Tokyo, Japan) or AVANCE 400 (Bruker, Billerica, MA, USA). Chemical shifts were expressed in ppm (δ) and were referenced to the residual solvent peak. Analytical thin layer chromatography (TLC) was carried out using precoated silica gel 60F254 (layer thickness, 0.25 mm; Merck, Darmstadt, Germany), and chromatography was performed using ZEOprep 60 silica gel (40–63 μ m; Zeochem, Lake Zurich, Switzerland). Mass spectra were recorded on a 6130 Single Quadrupole LC/MS (Agilent Technologies, Santa Clara, CA, USA) and High-resolution mass spectra (HRMS) were acquired under fast atom bombardments (FAB) condition on a JMS-700 MStation (JEOL, Tokyo, Japan). Preparative HPLC was performed on an YL9100 reversed-phase HPLC (Younglin, Anyang, South Korea).

4.1.1. Synthesis of the intermediates (**12a–b**)

4.1.1.1. 2-(4-Aminophenyl)-4H-1,3,4-oxadiazin-5(6H)-one (**12a**)

A solution of the hydrazide **8** (2.0 g, 11.04 mmol), bromoacetic acid (1.7 g, 12.14 mmol) and EDCI (3.2 g, 16.56 mmol) in DMF (28 mL) was stirred at room temperature for 1 h. The resulting mixture was diluted with EtOAc, washed with H₂O, and dried over Na₂SO₄. The crude solid was used for the next reaction without purification. DIEA (9.6 mL, 55.20 mmol) was added to a solution of the crude product **9** in DMF and the solution was stirred overnight at 70 °C. After cooling, the residue was taken up in H₂O and extracted with EtOAc. The combined extracts were dried over Na₂SO₄ and concentrated. The crude product was sonicated with MeOH for 5 minutes. The resulting precipitate was filtered to afford the corresponding 1,3,4-oxadiazin-5(6H)-one **10** (1.7 g, 68% in 2 steps). To the nitro compound **10** (0.8 g, 3.62 mmol) in DMF (9 mL) was added SnCl₂·2H₂O (3.3 g, 14.47 mmol). After stirring at 70 °C for 1 h, the reaction mixture was cooled down to room temperature and diluted with EtOAc, washed with saturated NaHCO₃ solution, and dried over Na₂SO₄. Intermediate **12a** was obtained by filtration with MeOH. Light brown solid (0.55 g, 80%). ¹H NMR (300 MHz,

DMSO- d_6) δ 10.78 (s, 1H), 7.42 (d, J = 8.6 Hz, 2H), 6.53 (d, J = 8.6 Hz, 2H), 5.66 (s, 2H), 4.64 (s, 2H).

4.1.1.2. 2-(4-Aminophenyl)-4-methyl-4H-1,3,4-oxadiazin-5(6H)-one (**12b**)

To a solution of NaH (4 mg, 0.09 mmol) in DMF (0.4 mL) was added compound **10** (20 mg, 0.09 mmol) in DMF (0.4 mL) at 0 °C and then the mixture was stirred at 0 °C for 0.5 h. After adding methyl iodide (6 μ L, 0.68 mmol) in DMF (0.2 mL), the mixture was stirred at room temperature for 1 h and was then quenched with H₂O. The reaction mixture was extracted with EtOAc, and dried over Na₂SO₄. The crude product was sonicated with DCM/Hexane to provide **11** (14 mg, 67%). To the nitro compound **11** (14 mg, 0.06 mmol) was added DMF (0.4 mL) and SnCl₂·2H₂O (4 mg, 0.09 mmol). After 1 h of stirring at 70 °C, the reaction mixture was cooled down to room temperature and diluted with saturated NaHCO₃ solution. The product was extracted with EtOAc, washed with brine, and dried over Na₂SO₄. Purification by silica gel column chromatography (DCM/MeOH = 80/1, R_f = 0.2) afforded **12b** as a light yellow solid (11 mg, 90%). ¹H NMR (300 MHz, DMSO- d_6) δ 7.45 (d, J = 8.4 Hz, 2H), 6.54 (d, J = 8.6 Hz, 2H), 5.72 (s, 2H), 4.69 (s, 2H), 3.20 (s, 3H).

4.1.2. Procedure for synthesis of **14–17**

4.1.2.1. 3-Chloro-*N*-[4-(5-oxo-5,6-dihydro-4H-1,3,4-oxadiazin-2-yl)phenyl]benzamide (**14**)

A solution of the 3-chlorobenzoic acid (100 mg, 0.64 mmol) in THF (3.2 mL) was treated at room temperature with few drops of DMF followed by oxalyl chloride (60 μ L, 0.71 mmol). The reaction mixture was stirred at 0 °C for 1 h and the volatiles were removed under reduced pressure. The crude mixture was dissolved in DMF (1.2 mL), and **12a** (50 mg, 0.26 mmol) was added followed by Et₃N (70 μ L, 0.52 mmol). The mixture was stirred at room temperature for 0.5 h, diluted with H₂O, extracted with EtOAc, and dried over Na₂SO₄. After adding MeOH, the precipitate was filtered and washed to afford the amide compound **14** as a light yellow solid (30 mg, 35% in 2 steps). Mp 265–266 °C; ¹H NMR (300 MHz, DMSO- d_6) δ 11.02 (s, 1H), 10.55 (s, 1H), 8.00 (s, 1H), 7.91 (d, J = 7.7

Hz, 1H), 7.87 (d, $J = 9.0$ Hz, 2H), 7.76 (d, $J = 8.8$ Hz, 2H), 7.68 (d, $J = 8.6$ Hz, 1H), 7.57 (t, $J = 7.9$ Hz, 1H), 4.76 (s, 2H); ^{13}C NMR (75 MHz, DMSO- d_6) δ 164.24, 161.09, 147.02, 140.96, 136.62, 133.19, 131.52, 130.39, 127.42, 126.60 (2C), 126.51, 124.98, 119.85 (2C), 64.54; LCMS (ESI) m/z 330 $[\text{M} + \text{H}]^+$; HRMS (FAB) m/z calcd for $\text{C}_{16}\text{H}_{13}\text{ClN}_3\text{O}_3$ $[\text{M} + \text{H}]^+$ 330.0645, found 330.0651.

4.1.2.2. 3-Chloro-*N*-(4-(5-oxo-5,6-dihydro-4H-1,3,4-oxadiazin-2-yl)phenyl)benzenesulfonamide (**15**)

To a solution of **12a** (20 mg, 0.11 mmol) in pyridine (0.5 mL) at 0 °C was added 3-chlorobenzenesulfonyl chloride (15 μL , 0.11 mmol). The reaction mixture was stirred at 0 °C for 1 h, acidified with 1 N HCl solution. The product was extracted with EtOAc, washed with brine, and dried over Na_2SO_4 . After adding DCM, the precipitate was filtered to afford the sulfonamide compound **15** as a light pink solid (22 mg, 60%). Mp 276 °C; ^1H NMR (300 MHz, DMSO- d_6) δ 10.99 (s, 1H), 10.75 (s, 1H), 7.78 (s, 1H), 7.71 (d, $J = 8.10$ Hz, 1H), 7.64 (d, $J = 8.8$ Hz, 2H), 7.61–7.56 (m, 2H), 7.17 (d, $J = 8.8$ Hz, 2H), 4.70 (s, 2H); ^{13}C NMR (75 MHz, DMSO- d_6) δ 161.04, 146.67, 141.00, 139.30, 133.87, 133.13, 131.44, 127.22 (2C), 126.14, 125.54, 125.35, 119.35 (2C), 64.52; LCMS (ESI) m/z 366 $[\text{M} + \text{H}]^+$; HRMS (FAB) m/z calcd for $\text{C}_{15}\text{H}_{13}\text{ClN}_3\text{O}_4\text{S}$ $[\text{M} + \text{H}]^+$ 366.0315, found 366.0324.

4.1.2.3. 1-(3-Chlorophenyl)-3-(4-(5-oxo-5,6-dihydro-4H-1,3,4-oxadiazin-2-yl)phenyl)urea (**16**)

The compound **12a** (20 mg, 0.11 mmol) was suspended in DCM/DMF (10/1, 1 mL) and 3-chlorophenyl isocyanate (20 μL , 0.16 mmol) was added. The mixture was stirred at room temperature for 5 h. The volatiles were removed under reduced pressure. MeOH was added and the solid was filtered to yield desired product as yellow solid (29 mg, 53%). Mp 308–309 °C; ^1H NMR (400 MHz, DMSO- d_6) δ 10.96 (s, 1H), 9.00 (s, 1H), 8.94 (s, 1H), 7.71–7.69 (m, 3H), 7.54 (d, $J = 8.8$ Hz, 2H), 7.33–7.28 (m, 2H), 7.02 (d, $J = 7.0$ Hz, 1H), 4.74 (s, 2H); ^{13}C NMR (100 MHz, DMSO- d_6)

δ 161.16, 152.13, 147.30, 141.67, 140.99, 133.20, 130.39, 126.91 (2C), 123.18, 121.68, 117.77 (2C), 117.71, 116.78, 64.54; LCMS (ESI) m/z 345 $[M + H]^+$; HRMS (FAB) m/z calcd for $C_{16}H_{14}ClN_4O_3$ $[M + H]^+$ 345.0754, found 345.0756.

4.1.2.4. 2-(4-((3-Chlorobenzyl)amino)phenyl)-4H-1,3,4-oxadiazin-5(6H)-one (**17**)

To a solution of **12a** (20 mg, 0.11 mmol) in 1 mL of MeOH was added 0.1 mL of acetic acid, followed by 3-chlorobenzaldehyde (20 μ L, 0.16 mmol) and NaCNBH₃ (13 mg, 0.21 mmol). The reaction mixture was stirred at room temperature for 2 h. The reaction mixture was diluted with NaHCO₃ in H₂O, extracted with EtOAc, and dried over Na₂SO₄. After adding DCM, the residue was filtered to afford **17** as yellow solid (25 mg, 75%). Mp 218–219 °C; ¹H NMR (300 MHz, DMSO-*d*₆) δ 10.79 (s, 1H), 7.46 (d, J = 8.8 Hz, 2H), 7.37 (s, 1H), 7.35–7.26 (m, 3H), 6.89 (t, J = 6.2 Hz, 1H), 6.58 (d, J = 8.8 Hz, 2H), 4.63 (s, 2H), 4.33 (d, J = 6.2 Hz, 2H); ¹³C NMR (75 MHz, DMSO-*d*₆) δ 161.30, 150.38, 148.36, 142.50, 133.05, 130.21, 127.44 (2C), 126.80, 126.68, 125.77, 116.85, 111.67 (2C), 64.44, 45.31; LCMS (ESI) m/z 316 $[M + H]^+$; HRMS (FAB) m/z calcd for $C_{16}H_{15}ClN_3O_2$ $[M + H]^+$ 316.0853, found 316.0854.

4.1.3. General procedure for the synthesis of diazo linker **18**

To a solution of **12a** (300 mg, 1.57 mmol) in MeOH (0.3 mL) were added H₂O₂ (0.8 mL), H₂O (0.6 mL) and MoO₃ (23 mg, 0.16 mmol). The resulting solution was stirred at room temperature for 5 d. H₂O was added, and the precipitate was filtered to yield desired product **13** as a yellow solid (270 mg, yield 85%). To a solution of **12a** or 3-substituted aniline (1 equiv.) in glacial acetic acid (0.4 mL) was added 3- or 4- substituted nitrosobenzene (1 equiv.) or **13** and the resulting mixture was stirred overnight at room temperature. The crude mixture was diluted with EtOAc, washed with saturated NaHCO₃ solution, and dried over Na₂SO₄. The precipitate in MeOH was filtered to afford diazo compounds **18a–e**.

4.1.3.1. (*E*)-2-(4-(Phenyldiazenyl)phenyl)-4H-1,3,4-oxadiazin-5(6*H*)-one (**18a**)

Light brown solid (yield 78%). Mp 257–259 °C; ¹H NMR (400 MHz, DMSO-*d*₆) δ 11.18 (s, 1H), 8.00–7.91 (m, 6H), 7.61 (m, 3H), 4.84 (s, 2H); ¹³C NMR (200 MHz, DMSO-*d*₆) δ 161.08, 152.72, 151.93, 146.38, 132.28, 131.94, 129.54 (2C), 127.10 (2C), 122.76 (2C), 122.70 (2C), 64.68; LCMS (ESI) *m/z* 281 [M + H]⁺; HRMS (FAB) *m/z* calcd for C₁₅H₁₂N₄O₂ [M + H]⁺ 281.1039, found 281.1045.

4.1.3.2. (*E*)-2-(4-((3-Fluorophenyl)diazenyl)phenyl)-4H-1,3,4-oxadiazin-5(6*H*)-one (**18b**)

Yellow solid (yield 69%). Mp 257–258 °C; ¹H NMR (400 MHz, DMSO-*d*₆) δ 11.19 (s, 1H), 8.02–8.00 (m, 4H), 7.82 (d, *J* = 8.0 Hz, 1H), 7.71–7.66 (m, 2H), 7.46 (td, *J* = 8.8, 2.0 Hz, 1H), 4.84 (s, 2H); ¹³C NMR (200 MHz, DMSO-*d*₆) δ 162.66 (d, *J* = 243.2 Hz), 161.06, 153.42 (d, *J* = 6.4 Hz), 152.43, 146.28, 132.73, 131.34 (d, *J* = 7.8 Hz), 127.12 (2C), 122.98 (2C), 120.56, 118.55 (d, *J* = 22.0 Hz), 107.73 (d, *J* = 22.2 Hz), 64.68; LCMS (ESI) *m/z* 299 [M + H]⁺; HRMS (FAB) *m/z* calcd for C₁₅H₁₁FN₄O₂ [M + H]⁺ 299.0944, found 299.0948.

4.1.3.3. 2-(4-((3-Chlorophenyl)diazenyl)phenyl)-4H-1,3,4-oxadiazin-5(6*H*)-one (**18c**)

Yellow solid (yield 83%). Mp 276–278 °C; ¹H NMR (300 MHz, DMSO-*d*₆) δ 11.19 (s, 1H), 7.98 (s, 4H), 7.93–7.90 (m, 2H), 7.67–7.65 (m, 2H), 4.83 (s, 2H); ¹³C NMR (75 MHz, DMSO-*d*₆) δ 161.01, 152.86, 152.44, 146.26, 134.19, 132.75, 131.32, 131.28, 127.09 (2C), 122.97 (2C), 122.62, 121.04, 64.66; LCMS (ESI) *m/z* 315 [M + H]⁺; HRMS (FAB) *m/z* calcd for C₁₅H₁₂ClN₄O₂ [M + H]⁺ 315.0649, found 315.0661.

4.1.3.4. (*E*)-2-(4-((4-Chlorophenyl)diazenyl)phenyl)-4H-1,3,4-oxadiazin-5(6*H*)-one (**18d**)

Light brown solid (yield 86%). Mp 275–277 °C; ^1H NMR (400 MHz, DMSO- d_6) δ 11.19 (s, 1H), 8.00–7.96 (m, 4H), 7.94 (d, $J = 8.8$ Hz, 2H), 7.69 (d, $J = 8.4$ Hz, 2H), 4.84 (s, 2H); ^{13}C NMR (125 MHz, DMSO- d_6) δ 161.06, 152.56, 150.48, 146.31, 136.43, 132.54, 129.68 (2C), 127.11 (2C), 124.37 (2C), 122.88 (2C), 64.68; LCMS (ESI) m/z 315 $[\text{M} + \text{H}]^+$; HRMS (FAB) m/z calcd for $\text{C}_{15}\text{H}_{11}\text{ClN}_4\text{O}_2$ $[\text{M} + \text{H}]^+$ 315.0649, found 315.0638.

4.1.3.5. (*E*)-2-(4-(*m*-Tolyldiazenyl)phenyl)-4H-1,3,4-oxadiazin-5(6*H*)-one (**18e**)

Brown solid (yield 37%). Mp 243–244 °C; ^1H NMR (400 MHz, DMSO- d_6) δ 11.18 (s, 1H), 7.96 (m, 4H), 7.73 (m, 2H), 7.51 (t, $J = 7.6$ Hz, 1H), 7.41 (d, $J = 7.6$ Hz, 1H), 4.83 (s, 2H), 2.44 (s, 3H); ^{13}C NMR (125 MHz, DMSO- d_6) δ 161.07, 152.75, 152.01, 146.39, 139.06, 132.57, 132.19, 129.32, 127.09 (2C), 122.69 (2C), 122.65, 120.41, 64.67, 20.85; LCMS (ESI) m/z 295 $[\text{M} + \text{H}]^+$; HRMS (FAB) m/z calcd for $\text{C}_{16}\text{H}_{14}\text{N}_4\text{O}_2$ $[\text{M} + \text{H}]^+$ 295.1195, found 295.1196.

4.1.4. General procedure for the preparation of imine **19a–f**

A mixture of amine compound **12a** (1 equiv.) and appropriate aldehyde (1 equiv.) in EtOH (1 mL) was refluxed overnight. After cooling, the precipitate was filtered to yield imine derivatives **19a–f**.

4.1.4.1. (*E*)-2-(4-(Benzylideneamino)phenyl)-4H-1,3,4-oxadiazin-5(6*H*)-one (**19a**)

Light brown solid (yield 45%). Mp 206–207 °C; ^1H NMR (400 MHz, DMSO- d_6) δ 11.05 (s, 1H), 8.66 (s, 1H), 7.97–7.94 (m, 2H), 7.82 (d, $J = 8.4$ Hz, 2H), 7.57–7.53 (m, 3H), 7.32 (d, $J = 8.8$ Hz, 2H), 4.78 (s, 2H); ^{13}C NMR (100 MHz, DMSO- d_6) δ 161.65, 161.12, 153.23, 147.02, 135.78, 131.76, 128.83 (4C), 127.25, 127.04 (2C), 121.19 (2C), 64.59; LCMS (ESI) m/z 280 $[\text{M} + \text{H}]^+$; HRMS (FAB) m/z calcd for $\text{C}_{16}\text{H}_{14}\text{N}_3\text{O}_2$ $[\text{M} + \text{H}]^+$ 280.1086, found 280.1098.

4.1.4.2. (*E*)-2-(4-((3-Fluorobenzylidene)amino)phenyl)-4H-1,3,4-oxadiazin-5(6*H*)-one (**19b**)

Light brown solid (yield 71%). Mp 200–202 °C; ¹H NMR (400 MHz, DMSO-*d*₆) δ 11.05 (s, 1H), 8.68 (s, 1H), 7.82 (d, *J* = 8.8 Hz, 2H), 7.79 (d, *J* = 8.0 Hz, 1H), 7.73 (d, *J* = 9.2 Hz, 1H), 7.58 (dd, *J* = 13.8, 8.0 Hz, 1H), 7.40 (td, *J* = 8.4, 2.8 Hz, 1H), 7.34 (d, *J* = 8.4 Hz, 2H), 4.78 (s, 2H); ¹³C NMR (100 MHz, DMSO-*d*₆) δ 162.37 (d, *J* = 243.1 Hz), 161.13, 160.48 (d, *J* = 2.8 Hz), 152.71, 146.97, 138.25 (d, *J* = 7.5 Hz), 130.99 (d, *J* = 7.9 Hz), 127.61, 127.08 (2C), 125.30 (d, *J* = 2.6 Hz), 121.28 (2C), 118.57 (d, *J* = 21.3 Hz), 114.50 (d, *J* = 21.9 Hz), 64.61; LCMS (ESI) *m/z* 298 [M + H]⁺; HRMS (FAB) *m/z* calcd for C₁₆H₁₃FN₃O₂ [M + H]⁺ 298.0992, found 298.1000.

4.1.4.3. (*E*)-2-(4-((3-Chlorobenzylidene)amino)phenyl)-4H-1,3,4-oxadiazin-5(6*H*)-one (**19c**)

Yellow solid (yield 61%). Mp 194–195 °C; ¹H NMR (300 MHz, DMSO-*d*₆) δ 11.07 (s, 1H), 8.67 (s, 1H), 7.98 (s, 1H), 7.91 (d, *J* = 7.3 Hz, 1H), 7.82 (d, *J* = 8.4 Hz, 2H), 7.64–7.54 (m, 2H), 7.34 (d, *J* = 8.4 Hz, 2H), 4.78 (s, 2H); ¹³C NMR (75 MHz, DMSO-*d*₆) δ 161.09, 160.29, 152.66, 146.93, 137.83, 133.67, 131.34, 130.77, 128.07, 127.62, 127.41, 127.05 (2C), 121.27 (2C), 64.59; LCMS (ESI) *m/z* 314 [M + H]⁺; HRMS (FAB) *m/z* calcd for C₁₆H₁₃ClN₃O₂ [M + H]⁺ 314.0696, found 314.0688.

4.1.4.4. (*E*)-2-(4-((4-Chlorobenzylidene)amino)phenyl)-4H-1,3,4-oxadiazin-5(6*H*)-one (**19d**)

Light brown solid (yield 80%). Mp 251–253 °C; ¹H NMR (300 MHz, DMSO-*d*₆) δ 11.06 (s, 1H), 8.68 (s, 1H), 7.96 (d, *J* = 8.6 Hz, 2H), 7.81 (d, *J* = 8.6 Hz, 2H), 7.60 (d, *J* = 8.4 Hz, 2H), 7.33 (d, *J* = 8.4 Hz, 2H), 4.78 (s, 2H); ¹³C NMR (75 MHz, DMSO-*d*₆) δ 161.39, 160.72, 153.14, 147.24, 136.63, 134.91, 130.71 (2C), 129.28 (2C), 127.74, 127.33 (2C), 121.55 (2C), 64.89; LCMS (ESI) *m/z* 314 [M + H]⁺; HRMS (FAB) *m/z* calcd for C₁₆H₁₃ClN₃O₂ [M + H]⁺ 314.0696, found 314.0689.

4.1.4.5. (*E*)-2-(4-((3-Methylbenzylidene)amino)phenyl)-4H-1,3,4-oxadiazin-5(6*H*)-one (**19e**)

Light yellow solid (yield 78%). Mp 218–220 °C; ^1H NMR (400 MHz, $\text{DMSO-}d_6$) δ 11.05 (s, 1H), 8.60 (s, 1H), 7.82 (d, $J = 8.8$ Hz, 2H), 7.77 (s, 1H), 7.73 (d, $J = 7.2$ Hz, 1H), 7.42 (t, $J = 7.6$ Hz, 1H), 7.37 (d, $J = 7.6$ Hz, 1H), 7.31 (d, $J = 8.8$ Hz, 2H), 4.78 (s, 2H), 2.38 (s, 3H); ^{13}C NMR (100 MHz, $\text{DMSO-}d_6$) δ 161.66, 161.12, 153.29, 147.04, 138.12, 135.77, 132.45, 129.01, 128.73, 127.20, 127.06 (2C), 126.35, 121.15 (2C), 64.59, 20.84; LCMS (ESI) m/z 294 $[\text{M} + \text{H}]^+$; HRMS (FAB) m/z calcd for $\text{C}_{17}\text{H}_{16}\text{N}_3\text{O}_2$ $[\text{M} + \text{H}]^+$ 294.1243, found 294.1239.

4.1.4.6. (*E*)-2-(4-((3-Chlorobenzylidene)amino)phenyl)-4-methyl-4H-1,3,4-oxadiazin-5(6H)-one (**19f**)

The compound was prepared from compound **12b**. Light yellow solid (yield 45%), Mp 152–153 °C; ^1H NMR (300 MHz, $\text{DMSO-}d_6$) δ 8.68 (s, 1H), 7.99 (s, 1H), 7.91 (d, $J = 7.3$ Hz, 1H), 7.84 (d, $J = 8.6$ Hz, 2H), 7.64–7.54 (m, 2H), 7.36 (d, $J = 8.4$ Hz, 2H), 4.83 (s, 2H), 3.28 (s, 3H); ^{13}C NMR (75 MHz, $\text{DMSO-}d_6$) δ 160.38, 159.09, 152.85, 147.23, 137.79, 133.66, 131.38, 130.78, 128.10, 127.42, 127.25 (2C), 127.08, 121.32 (2C), 64.70, 35.17; LCMS (ESI) m/z 328 $[\text{M} + \text{H}]^+$; HRMS (FAB) m/z calcd for $\text{C}_{17}\text{H}_{15}\text{ClN}_3\text{O}_2$ $[\text{M} + \text{H}]^+$ 328.0853, found 328.0861.

4.1.5. General procedure for preparation of **20**

The compound **14** (1 equiv.) in DMF (0.5 mL) was added dropwise to a suspension of NaH (1 equiv.) at 0 °C. The mixture was stirred at 0 °C for 0.5 h. 3-Bromopropionitrile (1 equiv.) or 2-chloroacetamide (1 equiv.) in DMF (0.2 mL) was added at 0 °C. The reaction was stirred at room temperature for 1 h, quenched with H_2O , and extracted with EtOAc. The organic phase was dried over Na_2SO_4 and concentrated.

4.1.5.1. 3-Chloro-*N*-(4-(4-(2-cyanoethyl)-5-oxo-5,6-dihydro-4H-1,3,4-oxadiazin-2-yl)phenyl)benzamide (**20a**)

Purification by silica gel chromatography (DCM/MeOH = 50/1, R_f = 0.25) afforded **20a** as a yellow solid (yield 95%). Mp 185–186 °C; ^1H NMR (400 MHz, DMSO- d_6) δ 10.56 (s, 1H), 8.02 (s, 1H), 7.94–7.89 (m, 3H), 7.84 (d, J = 8.8 Hz, 2H), 7.65 (d, J = 8.8 Hz, 1H), 7.58 (t, J = 7.6 Hz, 1H), 4.87 (s, 2H), 3.96 (t, J = 6.4 Hz, 2H), 2.94 (t, J = 6.4 Hz, 2H); ^{13}C NMR (100 MHz, DMSO- d_6) δ 164.29, 159.26, 148.11, 141.42, 136.56, 133.20, 131.56, 130.39, 127.45, 127.10 (2C), 126.54, 124.36, 119.80 (2C), 118.79, 64.65, 42.07, 15.81; LCMS (ESI) m/z 383 $[\text{M} + \text{H}]^+$; HRMS (FAB) m/z calcd for $\text{C}_{19}\text{H}_{16}\text{ClN}_4\text{O}_3$ $[\text{M} + \text{H}]^+$ 383.0911, found 383.0900.

4.1.5.2. *N*-(4-(4-(2-Amino-2-oxoethyl)-5-oxo-5,6-dihydro-4H-1,3,4-oxadiazin-2-yl)phenyl)-3-chlorobenzamide (**20b**)

Purification by filtration of slurry in MeOH afforded **20b** as a yellow solid (yield 72%). Mp 282–283 °C; ^1H NMR (400 MHz, DMSO- d_6) δ 10.56 (s, 1H), 8.02 (s, 1H), 7.90 (m, 3H), 7.78 (d, J = 8.8 Hz, 2H), 7.68 (d, J = 8.0 Hz, 1H), 7.58 (t, J = 8.0 Hz, 1H), 7.54 (brs, 1H), 7.21 (brs, 1H), 4.86 (s, 2H), 4.24 (s, 2H); ^{13}C NMR (75 MHz, DMSO- d_6) δ 168.61, 164.27, 159.39, 147.13, 141.25, 136.57, 133.20, 131.58, 130.42, 127.46, 126.87, 126.56, 124.52 (2C), 119.84 (2C), 64.69, 50.11; LCMS (ESI) m/z 387 $[\text{M} + \text{H}]^+$; HRMS (FAB) m/z calcd for $\text{C}_{18}\text{H}_{16}\text{ClN}_4\text{O}_4$ $[\text{M} + \text{H}]^+$ 387.0860, found 387.0868.

4.1.6. General synthesis of the compound **25**

To a suspension of NaH (1.5 equiv.) in THF was added the corresponding phosphate reagent (1.5 equiv.) in THF at 0 °C with stirring. After stirring for 0.5 h, methyl 4-formylbenzoate (1.0 equiv.) in THF was added dropwise to the reaction mixture. The resulting mixture was stirred at room temperature for 1 h, quenched with H_2O , extracted with EtOAc, and dried over Na_2SO_4 . Compound **22** was obtained by silica gel chromatography. To a product **22** in EtOH was added hydrazine monohydrate (15.0 equiv.) and was then refluxed overnight. After cooling, the resulting precipitate was filtered to give **23**. A solution of the compound **23**, bromoacetic acid (1.0 equiv.) and EDCI (1.0

equiv.) in DMF was stirred at room temperature for 1 h. The crude was diluted with EtOAc, washed with H₂O, and dried over Na₂SO₄. The resulting solid was used for the next reaction without purification. DIEA (5.0 equiv.) was added to a solution of the crude product **24** in DMF and then the mixture was stirred overnight at 70 °C. After cooling, the reaction mixture was diluted with H₂O, extracted with EtOAc, and dried over Na₂SO₄. Purification by preparative HPLC (H₂O with 0.1% TFA/ACN with 0.1% TFA, 50/50 to 95/5 in 35 minutes, flow rate = 1.0 mL/min) afforded the pure compound **25**.

4.1.6.1. (*E*)-2-(4-Styrylphenyl)-4H-1,3,4-oxadiazin-5(6*H*)-one (**25a**)

White solid (26% in 2 steps, HPLC purity: 100%). Mp 241–243 °C; ¹H NMR (800 MHz, DMSO-*d*₆) δ 11.06 (s, 1H), 7.77 (d, *J* = 8.8 Hz, 2H), 7.69 (d, *J* = 8.8 Hz, 2H), 7.63 (d, *J* = 8 Hz, 2H), 7.41–7.36 (m, 3H), 7.31–7.29 (m, 2H), 4.78 (s, 2H); ¹³C NMR (200 MHz, DMSO-*d*₆) δ 161.18, 147.04, 139.23, 136.75, 130.03, 128.76 (2C), 128.68, 128.02, 127.50, 126.69 (2C), 126.56 (2C), 126.33 (2C), 64.59; LCMS (ESI) *m/z* 279 [M + H]⁺; HRMS (FAB) *m/z* calcd for C₁₇H₁₅N₂O₂ [M + H]⁺ 279.1134, found 279.1125.

4.1.6.2. (*E*)-2-(4-(3-Fluorostyryl)phenyl)-4H-1,3,4-oxadiazin-5(6*H*)-one (**25b**)

White solid (25% in 2 steps, HPLC purity: 94%). Mp 219–221 °C; ¹H NMR (300 MHz, DMSO-*d*₆) δ 11.06 (s, 1H), 7.78 (d, *J* = 8.6 Hz, 2H), 7.68 (d, *J* = 8.4 Hz, 2H), 7.51–7.37 (m, 5H), 7.11 (m, 1H), 4.77 (s, 2H); ¹³C NMR (75 MHz, DMSO-*d*₆) δ 162.54 (d, *J* = 241.4 Hz), 161.09, 146.90, 139.43 (d, *J* = 8.0 Hz), 138.78, 130.58 (d, *J* = 8.3 Hz), 129.04, 128.97, 128.70 (d, *J* = 2.6 Hz), 126.69 (2C), 126.29 (2C), 123.10 (d, *J* = 2.3 Hz), 114.56 (d, *J* = 20.7 Hz), 112.63 (d, *J* = 21.6 Hz), 64.57; LCMS (ESI) *m/z* 297 [M + H]⁺; HRMS (FAB) *m/z* calcd for C₁₇H₁₃FN₂O₂ [M + H]⁺ 296.0961, found 296.0964.

4.1.6.3. (*E*)-2-(4-(3-Chlorostyryl)phenyl)-4H-1,3,4-oxadiazin-5(6*H*)-one (**25c**)

White solid (26% in 2 steps, HPLC purity: 100%). Mp 207–208 °C; ^1H NMR (300 MHz, $\text{DMSO-}d_6$) δ 11.07 (s, 1H), 7.78 (d, $J = 8.6$ Hz, 2H), 7.72 (s, 1H), 7.68 (d, $J = 8.4$ Hz, 2H), 7.58 (d, $J = 7.9$ Hz, 1H), 7.42 (d, $J = 8.2$ Hz, 1H), 7.32 (m, 3H), 4.77 (s, 2H); ^{13}C NMR (75 MHz, $\text{DMSO-}d_6$) δ 161.11, 146.91, 139.09, 138.80, 133.57, 130.51, 129.17, 129.00, 128.41, 127.55, 126.73 (2C), 126.30 (2C), 126.06, 125.38, 64.58; LCMS (ESI) m/z 313 $[\text{M} + \text{H}]^+$; HRMS (FAB) m/z calcd for $\text{C}_{17}\text{H}_{14}\text{ClN}_2\text{O}_2$ $[\text{M} + \text{H}]^+$ 313.0744, found 313.0751.

4.1.6.4. (*E*)-2-(4-(4-Chlorostyryl)phenyl)-4H-1,3,4-oxadiazin-5(6*H*)-one (**25d**)

White solid (25% in 2 steps, HPLC purity: 100%). Mp 234–235 °C; ^1H NMR (400 MHz, $\text{DMSO-}d_6$) δ 11.07 (s, 1H), 7.77 (d, $J = 8.4$ Hz, 2H), 7.68 (d, $J = 8.8$ Hz, 2H), 7.65 (d, $J = 8.8$ Hz, 2H), 7.44 (d, $J = 8.4$ Hz, 2H), 7.36 (d, $J = 16.4$ Hz, 1H), 7.31 (d, $J = 16.4$ Hz, 1H), 4.77 (s, 2H); ^{13}C NMR (75 MHz, $\text{DMSO-}d_6$) δ 161.10, 146.94, 138.93, 135.71, 132.23, 128.83, 128.70 (2C), 128.63, 128.33, 128.28 (2C), 126.61 (2C), 126.28 (2C), 64.57; LCMS (ESI) m/z 313 $[\text{M} + \text{H}]^+$; HRMS (FAB) m/z calcd for $\text{C}_{17}\text{H}_{13}\text{ClN}_2\text{O}_2$ $[\text{M} + \text{H}]^+$ 312.0666, found 312.0662.

4.1.6.5. (*E*)-2-(4-(3-Methylstyryl)phenyl)-4H-1,3,4-oxadiazin-5(6*H*)-one (**25e**)

Light brown solid (25% in 2 steps, HPLC purity: 96%). Mp 170–172 °C; ^1H NMR (300 MHz, $\text{DMSO-}d_6$) δ 11.05 (s, 1H), 7.76 (d, $J = 8.3$ Hz, 2H), 7.67 (d, $J = 8.4$ Hz, 2H), 7.45 (s, 1H), 7.41 (d, $J = 7.9$ Hz, 1H), 7.30–7.24 (m, 3H), 7.10 (d, $J = 7.7$ Hz, 1H), 4.77 (s, 2H), 2.33 (s, 3H); ^{13}C NMR (75 MHz, $\text{DMSO-}d_6$) δ 161.16, 147.04, 139.28, 137.81, 136.67, 130.08, 128.63 (3C), 127.30, 127.14, 126.49 (2C), 126.31 (2C), 124.01, 64.58, 20.99; LCMS (ESI) m/z 293 $[\text{M} + \text{H}]^+$; HRMS (FAB) m/z calcd for $\text{C}_{18}\text{H}_{17}\text{N}_2\text{O}_2$ $[\text{M} + \text{H}]^+$ 293.1290, found 293.1287.

4.2. Human MAO inhibition assay

Recombinant human MAO-A and MAO-B were purchased from Sigma-Aldrich (St. Louis, MO, USA). Inhibition of enzyme activity was measured using Amplex Red MAO assay kit (Molecular probes, Eugene, Oregon, USA). Briefly, assays are based on the detection of H₂O₂ via an oxidative deamination reaction of the substrate p-tyramine. The production of H₂O₂ was measured in a horseradish peroxidase coupled reaction using Amplex red reagent, highly sensitive and stable probe for H₂O₂. The assay condition was established according to the manufacturer's instruction with the modifications described below. The experiments were performed in 384 well black bottom plate in a volume of 100 μ L at room temperature. To 10 μ L of sodium phosphate buffer (0.05 M, pH 7.4) containing various concentrations of test compounds were added 0.25 μ g MAO-A or 1.25 μ g MAO-B in 40 μ L sodium phosphate buffer and then incubated for 30 min at room temperature. The enzymatic reaction was started by adding 50 μ L of a sodium phosphate buffer containing 200 μ M Amplex red reagent, 1 U/mL horseradish peroxidase, and 0.5 mM p-tyramine. The samples were incubated for 30 min at room temperature protected from light. The subsequent production of resorufin was detected using a microplate reader (Mithras LB 940 Multimode Microplate Reader, Berthold Technologies, Bad Wildbad, Germany) with an excitation at 545 nm and emission at 590 nm. Enzyme inhibition was initially determined at a certain concentration (for MAO-A, 10 or 100 μ M; for MAO-B, 1 or 10 μ M) and IC₅₀ of potent compounds was calculated by nonlinear regression using GraphPad Prism version 5.0 (San Diego, CA, USA). Each IC₅₀ value is the mean from more than three experiments ($n \geq 3$).

4.3. Time-dependent inhibition

Compound **18a**, **25b**, **19c**, and **19e** were preincubated for 0, 15, 30, 60 min at 37 °C with recombinant hMAO-B (1.25 μ g) in sodium phosphate buffer (0.05 M, pH 7.4). The concentrations of the tested compounds were 3-fold of the measured IC₅₀ values (pargyline: 780 nM) for the inhibition of MAO-B. The enzymatic reaction was started by adding 50 μ L of a sodium phosphate buffer containing 200 μ M Amplex red reagent, 1.5 U/mL horseradish peroxidase, and 0.5 mM p-

tyramine. The samples were incubated for 30 min at 37 °C protected from light. The subsequent production of resorufin was detected using a microplate reader (Mithras LB 940 Multimode Microplate Reader, Berthold Technologies, Bad Wildbad, Germany) with an excitation at 545 nm and emission at 590 nm. Data are expressed as the mean \pm SEM of three independent experiments.

4.4. Cell culture and cytotoxicity assay

PC-12 cells were grown in RPMI-1640 supplemented with 10% horse serum, 5% fetal bovine serum (FBS), and 1% antibiotic solution at 37 °C in an atmosphere of 5% CO₂. PC-12 Adh cells were grown in F12K supplemented with 15% horse serum, 2.5% FBS and 1% antibiotic solution at 37 °C in an atmosphere of 5% CO₂. SH-SY5Y cells were grown in Minimum Essential Medium Eagle (MEM) supplemented with 10% FBS and 1% antibiotic solution at 37 °C in an atmosphere of 5% CO₂. The viability of neuroblastoma cells (PC-12, PC-12 Adh, and SH-SY5Y) was investigated using the EZ-Cytox cell viability assay kit (WST, water-soluble tetrazolium salt method). The experiment was performed according to the manufacturer's instruction. Cells were seeded on 96 well plate (100 μ L) in an appropriate density (PC-12 and SH-SY5Y: 10000 cells/well, PC-12 Adh: 6000 cells/well). After 24 h, compounds **18a**, **25b**, **19c**, and **19e** (10 and 50 μ M) were treated to each well, and the resulting plates were incubated for an additional 24 h. WST reagent (10 μ L) was added to each well and the plate was incubated for 4 h at 37 °C under 5% CO₂. Absorbance at 450 nm was measured by microplate reader (Mithras LB 940 Multimode Microplate Reader, Berthold Technologies, Bad Wildbad, Germany). These results were expressed as a percentage, relative to untreated control incubations (n = 3 in triplicate).

4.5. General procedure for molecular docking.

Sybyl-X 2.1.1 (Tripos Inc, St Louis, MO) was used to carry out molecular docking studies. The X-ray cocrystal structure of human MAO-B (PDB ID: 2V5Z) complexed with safinamide was selected

as template and the chain B of PDB structure was prepared for docking studies. The docking ligands were built using ChemBioDraw ultra 13.0 and prepared by generating 3D conformations from 2D structures using Quick 3D protocol in Sybyl-X 2.1.1. The energy minimization of protein was conducted using gradient minimization (Powell's method) with the MMFF94 force field until the RMSD was lower than 0.001 kcal/mol·Å. The original ligand and all the water molecules were removed. The protomol was generated on the basis of ligand mode (threshold of 0.5 Å and bloat of 0 Å). Docking runs were performed through Surflex-Dock GeomX mode with the flexible hydrogens and heavy atoms of the protein. Docking performance was validated by examination of the RMSD of the re-docked structure compared to the original pose (RMSD, 0.67 Å). Molecular interactions between ligand and protein were further analyzed using BIOVIA Discovery Studio 2016 Visualizer (Dassault Systèmes, San Diego, CA).

4.6. Theoretical evaluation of physicochemical properties

Physicochemical properties of the compounds were calculated by using BIOVIA Discovery Studio 2016 (Dassault Systèmes, San Diego, CA).

Acknowledgment

This work was supported by the National Research Foundation of Korea (NRF) grants funded by the Korean government (MSIP) (2009-0083533 and NRF-2015R1A2A2A01007646).

Appendix A. Supplementary data

References

- [1] G.G. Collins, M. Sandler, E.D. Williams, M.B. Youdim, Multiple forms of human brain mitochondrial monoamine oxidase, *Nature*, 225 (1970) 817-820.
- [2] M.B. Youdim, G.G. Collins, M. Sandler, A.B. Bevan Jones, C.M. Pare, W.J. Nicholson, Human brain monoamine oxidase: multiple forms and selective inhibitors, *Nature*, 236 (1972) 225-228.
- [3] M.D. Houslay, K.F. Tipton, A kinetic evaluation of monoamine oxidase activity in rat liver mitochondrial outer membranes, *Biochem J*, 139 (1974) 645-652.
- [4] C.J. Fowler, M.S. Benedetti, The metabolism of dopamine by both forms of monoamine oxidase in the rat brain and its inhibition by cimaxatone, *Journal of neurochemistry*, 40 (1983) 1534-1541.
- [5] J.C. Shih, K. Chen, M.J. Ridd, Monoamine oxidase: from genes to behavior, *Annual review of neuroscience*, 22 (1999) 197-217.
- [6] C.H. Donnelly, D.L. Murphy, Substrate- and inhibitor-related characteristics of human platelet monoamine oxidase, *Biochem Pharmacol*, 26 (1977) 853-858.
- [7] L.W. Thorpe, K.N. Westlund, L.M. Kochersperger, C.W. Abell, R.M. Denney, Immunocytochemical localization of monoamine oxidases A and B in human peripheral tissues and brain, *J Histochem Cytochem*, 35 (1987) 23-32.
- [8] J. Saura, R. Kettler, M. Da Prada, J.G. Richards, Quantitative enzyme radioautography with 3H-Ro 41-1049 and 3H-Ro 19-6327 in vitro: localization and abundance of MAO-A and MAO-B in rat CNS, peripheral organs, and human brain, *J Neurosci*, 12 (1992) 1977-1999.
- [9] M.B. Youdim, D. Edmondson, K.F. Tipton, The therapeutic potential of monoamine oxidase inhibitors, *Nat Rev Neurosci*, 7 (2006) 295-309.
- [10] B. Strydom, J.J. Bergh, J.P. Petzer, 8-Aryl- and alkyloxycaffeine analogues as inhibitors of monoamine oxidase, *European journal of medicinal chemistry*, 46 (2011) 3474-3485.
- [11] C. Mattsson, P. Svensson, C. Sonesson, A novel series of 6-substituted 3-(pyrrolidin-1-ylmethyl)chromen-2-ones as selective monoamine oxidase (MAO) A inhibitors, *European journal of medicinal chemistry*, 73 (2014) 177-186.
- [12] P.B. Huleatt, M.L. Khoo, Y.Y. Chua, T.W. Tan, R.S. Liew, B. Balogh, R. Deme, F. Goloncser, K. Magyar, D.P. Sheela, H.K. Ho, B. Sperlagh, P. Matyus, C.L. Chai, Novel arylalkenylpropargylamines as neuroprotective, potent, and selective monoamine oxidase B inhibitors for the treatment of Parkinson's disease, *Journal of medicinal chemistry*, 58 (2015) 1400-1419.
- [13] S.S. Xie, J. Chen, X.R. Li, T. Su, Y.L. Wang, Z.R. Wang, L. Huang, X.S. Li, Synthesis and evaluation of selegiline derivatives as monoamine oxidase inhibitor, antioxidant and metal chelator against Alzheimer's disease, *Bioorganic & medicinal chemistry*, 23 (2015) 3722-3729.
- [14] V.N. Badavath, I. Baysal, G. Ucar, B.N. Sinha, V. Jayaprakash, Monoamine Oxidase Inhibitory Activity of Novel Pyrazoline Analogues: Curcumin Based Design and Synthesis, *ACS medicinal chemistry letters*, 7 (2016) 56-61.
- [15] S. Distinto, R. Meleddu, M. Yanez, R. Cirilli, G. Bianco, M.L. Sanna, A. Arridu, P. Cossu, F. Cottiglia, C. Faggi, F. Ortuso, S. Alcaro, E. Maccioni, Drug design, synthesis, in vitro and in silico evaluation of selective monoaminoxidase B inhibitors based on 3-acetyl-2-dichlorophenyl-5-aryl-2,3-dihydro-1,3,4-oxadiazole chemical scaffold, *European journal of medicinal chemistry*, 108 (2016) 542-552.

- [16] Z. Fisar, Drugs related to monoamine oxidase activity, *Progress in neuro-psychopharmacology & biological psychiatry*, 69 (2016) 112-124.
- [17] R.K. Tripathi, S. Krishnamurthy, S.R. Ayyannan, Discovery of 3-Hydroxy-3-phenacyloxindole Analogues of Isatin as Potential Monoamine Oxidase Inhibitors, *ChemMedChem*, 11 (2016) 119-132.
- [18] P. Gareri, U. Falconi, P. De Fazio, G. De Sarro, Conventional and new antidepressant drugs in the elderly, *Prog Neurobiol*, 61 (2000) 353-396.
- [19] K.I. Shulman, N. Herrmann, S.E. Walker, Current place of monoamine oxidase inhibitors in the treatment of depression, *CNS drugs*, 27 (2013) 789-797.
- [20] M. Schachter, C.D. Marsden, J.D. Parkes, P. Jenner, B. Testa, Deprenyl in the management of response fluctuations in patients with Parkinson's disease on levodopa, *Journal of neurology, neurosurgery, and psychiatry*, 43 (1980) 1016-1021.
- [21] J.M. Rabey, I. Sagi, M. Huberman, E. Melamed, A. Korczyn, N. Giladi, R. Inzelberg, R. Djaldetti, C. Klein, G. Berecz, G. Rasagiline Study, Rasagiline mesylate, a new MAO-B inhibitor for the treatment of Parkinson's disease: a double-blind study as adjunctive therapy to levodopa, *Clinical neuropharmacology*, 23 (2000) 324-330.
- [22] A.H. Schapira, F. Stocchi, R. Borgohain, M. Onofrj, M. Bhatt, P. Lorenzana, V. Lucini, R. Giuliani, R. Anand, I. Study, Long-term efficacy and safety of safinamide as add-on therapy in early Parkinson's disease, *Eur J Neurol*, 20 (2013) 271-280.
- [23] D. Robakis, S. Fahn, Defining the Role of the Monoamine Oxidase-B Inhibitors for Parkinson's Disease, *CNS drugs*, 29 (2015) 433-441.
- [24] J.S. Fowler, N.D. Volkow, G.J. Wang, J. Logan, N. Pappas, C. Shea, R. MacGregor, Age-related increases in brain monoamine oxidase B in living healthy human subjects, *Neurobiology of aging*, 18 (1997) 431-435.
- [25] J. Saura, N. Andres, C. Andrade, J. Ojuel, K. Eriksson, N. Mahy, Biphasic and region-specific MAO-B response to aging in normal human brain, *Neurobiology of aging*, 18 (1997) 497-507.
- [26] P. Levitt, J.E. Pinter, X.O. Breakefield, Immunocytochemical demonstration of monoamine oxidase B in brain astrocytes and serotonergic neurons, *Proc Natl Acad Sci U S A*, 79 (1982) 6385-6389.
- [27] M.B. Youdim, Y.S. Bakhle, Monoamine oxidase: isoforms and inhibitors in Parkinson's disease and depressive illness, *British journal of pharmacology*, 147 Suppl 1 (2006) S287-296.
- [28] M. Bortolato, K. Chen, J.C. Shih, Monoamine oxidase inactivation: from pathophysiology to therapeutics, *Adv Drug Deliv Rev*, 60 (2008) 1527-1533.
- [29] P. Riederer, K. Jellinger, Neurochemical Insights into Monoamine-Oxidase Inhibitors, with Special Reference to Deprenyl (Selegiline), *Acta Neurol Scand*, 68 (1983) 43-55.
- [30] F.S. Glazener, P.K. Johnson, W.A. Morgan, J.M. Simpson, Pargyline Cheese + Acute Hypertension, *Jama-J Am Med Assoc*, 188 (1964) 754-&.
- [31] Blackwel.B, L.A. Mabbitt, Tyramine in Cheese Related to Hypertensive Crises after Monoamine-Oxidase Inhibition, *Lancet*, 1 (1965) 938-&.
- [32] J.D. Elsworth, V. Glover, G.P. Reynolds, M. Sandler, A.J. Lees, P. Phuapradit, K.M. Shaw, G.M. Stern, P. Kumar, Deprenyl Administration in Man - Selective Monoamine Oxidase-B Inhibitor without Cheese Effect, *Psychopharmacology*, 57 (1978) 33-38.

- [33] J.P. Finberg, M. Tenne, Relationship between tyramine potentiation and selective inhibition of monoamine oxidase types A and B in the rat vas deferens, *British journal of pharmacology*, 77 (1982) 13-21.
- [34] M.B. Youdim, M. Weinstock, Therapeutic applications of selective and non-selective inhibitors of monoamine oxidase A and B that do not cause significant tyramine potentiation, *Neurotoxicology*, 25 (2004) 243-250.
- [35] L. Pisani, G. Muncipinto, T.F. Miscioscia, O. Nicolotti, F. Leonetti, M. Catto, C. Caccia, P. Salvati, R. Soto-Otero, E. Mendez-Alvarez, C. Passeleu, A. Carotti, Discovery of a Novel Class of Potent Coumarin Monoamine Oxidase B Inhibitors: Development and Biopharmacological Profiling of 7-[(3-Chlorobenzyl)oxy]-4-[(methylamino)methyl]-2H-chromen-2-one Methanesulfonate (NW-1772) as a Highly Potent, Selective, Reversible, and Orally Active Monoamine Oxidase B Inhibitor, *Journal of medicinal chemistry*, 52 (2009) 6685-6706.
- [36] J.P.M. Finberg, K. Gillman, Selective Inhibitors of Monoamine Oxidase Type B and the "Cheese Effect", *International Review of Neurobiology*, 100 (2011) 169-190.
- [37] M.J. Matos, C. Teran, Y. Perez-Castillo, E. Uriarte, L. Santana, D. Vina, Synthesis and study of a series of 3-arylcoumarins as potent and selective monoamine oxidase B inhibitors, *Journal of medicinal chemistry*, 54 (2011) 7127-7137.
- [38] N.T. Tzvetkov, S. Hinz, P. Kuppers, M. Gastreich, C.E. Muller, Indazole- and Indole-5-carboxamides: Selective and Reversible Monoamine Oxidase B Inhibitors with Subnanomolar Potency, *Journal of medicinal chemistry*, 57 (2014) 6679-6703.
- [39] F. Cagide, T. Silva, J. Reis, A. Gaspar, F. Borges, L.R. Gomes, J.N. Low, Discovery of two new classes of potent monoamine oxidase-B inhibitors by tricky chemistry, *Chemical Communications*, 51 (2015) 2832-2835.
- [40] S. Carradori, R. Silvestri, New Frontiers in Selective Human MAO-B Inhibitors, *Journal of medicinal chemistry*, (2015).
- [41] J.W. Choi, B.K. Jang, N.C. Cho, J.H. Park, S.K. Yeon, E.J. Ju, Y.S. Lee, G. Han, A.N. Pae, D.J. Kim, K.D. Park, Synthesis of a series of unsaturated ketone derivatives as selective and reversible monoamine oxidase inhibitors, *Bioorganic & medicinal chemistry*, 23 (2015) 6486-6496.
- [42] N. Desideri, L. Proietti Monaco, R. Fioravanti, M. Biava, M. Yanez, S. Alcaro, F. Ortuso, (E)-3-Heteroarylidenochroman-4-ones as potent and selective monoamine oxidase-B inhibitors, *European journal of medicinal chemistry*, 117 (2016) 292-300.
- [43] J.P. Johnston, Some observations upon a new inhibitor of monoamine oxidase in brain tissue, *Biochem Pharmacol*, 17 (1968) 1285-1297.
- [44] F. Chimenti, D. Secci, A. Bolasco, P. Chimenti, A. Granese, S. Carradori, M. D'Ascenzio, M. Yanez, F. Orallo, Synthesis and selective inhibition of human monoamine oxidases of a large scaffold of (4,5-substituted-thiazol-2-yl)hydrazones, *Medchemcomm*, 1 (2010) 61-72.
- [45] L.H. Mu, B. Wang, H.Y. Ren, P. Liu, D.H. Guo, F.M. Wang, L. Bai, Y.S. Guo, Synthesis and inhibitory effect of piperine derivatives on monoamine oxidase, *Bioorg Med Chem Lett*, 22 (2012) 3343-3348.
- [46] L. Ambrozi, W. Birkmayer, P. Riederer, M.B. Youdim, L-dopa and (-)-deprenil in the treatment of Parkinson's disease: a long-term study [proceedings], *British journal of pharmacology*, 58 (1976) 423P-424P.

- [47] M.B. Youdim, A. Gross, J.P. Finberg, Rasagiline [N-propargyl-1R(+)-aminoindan], a selective and potent inhibitor of mitochondrial monoamine oxidase B, *British journal of pharmacology*, 132 (2001) 500-506.
- [48] P. Riederer, L. Lachenmayer, Selegiline's neuroprotective capacity revisited, *J Neural Transm (Vienna)*, 110 (2003) 1273-1278.
- [49] S. Mandel, O. Weinreb, T. Amit, M.B. Youdim, Mechanism of neuroprotective action of the anti-Parkinson drug rasagiline and its derivatives, *Brain Res Brain Res Rev*, 48 (2005) 379-387.
- [50] F. Leonetti, C. Capaldi, L. Pisani, O. Nicolotti, G. Muncipinto, A. Stefanachi, S. Cellamare, C. Caccia, A. Carotti, Solid-phase synthesis and insights into structure-activity relationships of safinamide analogues as potent and selective inhibitors of type B monoamine oxidase, *Journal of medicinal chemistry*, 50 (2007) 4909-4916.
- [51] M.M. Alam, S.C. Lee, Y. Jung, H.J. Yun, H.Y. Min, H.J. Lee, P.C. Pham, J. Moon, D.I. Kwon, B. Lim, Y.G. Suh, J. Lee, H.Y. Lee, Novel C6-substituted 1,3,4-oxadiazinones as potential anti-cancer agents, *Oncotarget*, 6 (2015) 40598-40610.
- [52] F. Mazouz, L. Lebreton, R. Milcent, C. Burstein, Inhibition of Monoamine-Oxidase Type-a and Type-B by 2-Aryl-4h-1,3,4-Oxadiazin-5(6h)-One Derivatives, *European journal of medicinal chemistry*, 23 (1988) 441-451.
- [53] F. Mazouz, L. Lebreton, R. Milcent, C. Burstein, 5-Aryl-1,3,4-Oxadiazol-2(3h)-One Derivatives and Sulfur Analogs as New Selective and Competitive Monoamine-Oxidase Type-B Inhibitors, *European journal of medicinal chemistry*, 25 (1990) 659-671.
- [54] F. Mazouz, S. Gueddari, C. Burstein, D. Mansuy, R. Milcent, 5-[4-(Benzyloxy)Phenyl]-1,3,4-Oxadiazol-2(3h)-One Derivatives and Related Analogs - New Reversible, Highly Potent, and Selective Monoamine-Oxidase Type-B Inhibitors, *Journal of medicinal chemistry*, 36 (1993) 1157-1167.
- [55] S.Y. Ke, X.H. Qian, F.Y. Liu, N. Wang, Q. Yang, Z. Li, Novel 4H-1,3,4-oxadiazin-5(6H)-ones with hydrophobic and long alkyl chains: Design, synthesis, and bioactive diversity on inhibition of monoamine oxidase, chitin biosynthesis and tumor cell, *European journal of medicinal chemistry*, 44 (2009) 2113-2121.
- [56] L. De Colibus, M. Li, C. Binda, A. Lustig, D.E. Edmondson, A. Mattevi, Three-dimensional structure of human monoamine oxidase A (MAO A): relation to the structures of rat MAO A and human MAO B, *Proc Natl Acad Sci U S A*, 102 (2005) 12684-12689.
- [57] C. Binda, J. Wang, L. Pisani, C. Caccia, A. Carotti, P. Salvati, D.E. Edmondson, A. Mattevi, Structures of human monoamine oxidase B complexes with selective noncovalent inhibitors: safinamide and coumarin analogs, *Journal of medicinal chemistry*, 50 (2007) 5848-5852.
- [58] C. Binda, P. Newton-Vinson, F. Hubalek, D.E. Edmondson, A. Mattevi, Structure of human monoamine oxidase B, a drug target for the treatment of neurological disorders, *Nature structural biology*, 9 (2002) 22-26.
- [59] A. Holt, D.F. Sharman, G.B. Baker, M.M. Palcic, A continuous spectrophotometric assay for monoamine oxidase and related enzymes in tissue homogenates, *Anal Biochem*, 244 (1997) 384-392.
- [60] F. Chimenti, R. Fioravanti, A. Bolasco, P. Chimenti, D. Secci, F. Rossi, M. Yanez, F. Orallo, F. Ortuso, S. Alcaro, Chalcones: A Valid Scaffold for Monoamine Oxidases Inhibitors, *Journal of medicinal chemistry*, 52 (2009) 2818-2824.

- [61] L. Legoabe, J. Kruger, A. Petzer, J.J. Bergh, J.P. Petzer, Monoamine oxidase inhibition by selected anilide derivatives, *European journal of medicinal chemistry*, 46 (2011) 5162-5174.
- [62] R.K. Tripathi, O. Goshain, S.R. Ayyannan, Design, synthesis, in vitro MAO-B inhibitory evaluation, and computational studies of some 6-nitrobenzothiazole-derived semicarbazones, *ChemMedChem*, 8 (2013) 462-474.
- [63] C.A. Lipinski, F. Lombardo, B.W. Dominy, P.J. Feeney, Experimental and computational approaches to estimate solubility and permeability in drug discovery and development settings, *Advanced Drug Delivery Reviews*, 23 (1997) 3-25.
- [64] D.E. Clark, Rapid calculation of polar molecular surface area and its application to the prediction of transport phenomena. 1. Prediction of intestinal absorption, *J Pharm Sci-U.S.*, 88 (1999) 807-814.
- [65] S.A. Hitchcock, L.D. Pennington, Structure-brain exposure relationships, *Journal of medicinal chemistry*, 49 (2006) 7559-7583.

Discovery of highly selective and potent monoamine oxidase B inhibitors: contribution of additional phenyl rings introduced into 2-aryl-1,3,4-oxadiazin-5(6H)-one

Jungeun Lee, Yeongcheol Lee, So Jung Park, Joohee Lee, Yeong Shik Kim, Young-Ger Suh,
and Jeeyeon Lee*

*College of Pharmacy and Research Institute of Pharmaceutical Sciences, Seoul National
University, Seoul 08826, Korea*

* Corresponding author.

E-mail address: jyleeut@snu.ac.kr (J. Lee).

Highlights

- Linear analogs of 2-aryl-1,3,4-oxadiazin-5(6H)-one were designed and synthesized.
- Compounds 18a, 18b, 18e and 25b potently inhibited MAO-B with excellent SIs.
- Optimizing the linker between two aromatic rings is a key element in MAO-B inhibition.